Granular media: some ideas from statistical physics

J.P. Bouchaud
Service de Physique de l'Etat Condensé,
CEA, Orme des Merisiers,
91191 Gif-sur-Yvette, Cedex France.

These lecture notes cover the statics and glassy dynamics of granular media. Most of the lectures were in fact devoted to 'force propagation' models. We discuss the experimental and theoretical motivations for these approaches, and their conceptual connections with Edwards' thermodynamical analogy. One of the distinctive feature of granular media (common to many other 'jammed' systems) is indeed the large number of metastable states that are macroscopically equivalent. We present in detail the (scalar) q-model and its tensorial generalization, that aim at modelling the existence of force chains and arching effects without introducing any displacement field. The contrast between the hyperbolic equations obtained within this line of thought and elliptic (elastic) equations is emphasized. The rôle of disorder on these hyperbolic equations is studied in details using perturbative and diagrammatic methods. Recent (strong disorder) force chain network models are reviewed, and compared with the experimental determination of the force 'response function' in granular materials. We briefly discuss several issues (such as isostaticity and generic marginality) and open problems. At the end of these notes, we also discuss the basic dynamical properties of *weakly tapped* granular assemblies, and stress the phenomenological analogies with other glassy materials. Simple models that account for slow compaction and dynamical heterogeneities are presented, that are inspired by 'free-volume' ideas and Edwards' assumption. A connection with the theory of fluctuating random surfaces, also noted recently by Castillo et al., is suggested. Finally, we discuss how the 'trap model' can be adapted to granular materials, such that more subtle 'memory' effects can be accounted for.

arXiv:cond-mat/0211196v2 24 Dec 2002

I. INTRODUCTION

A. Basic phenomenology

Although granular materials are made of classical particles of macroscopic size, they exhibit a host of interesting and sometimes counter-intuitive properties, which are of interest both to the academic community and for industrial applications: enormous amounts of 'granular assemblies' are routinely handled (stored, transported, mixed together, etc.) The reason why these systems are still not fully understood yet is that they require a proper statistical treatment of collective effects. Although the physics at the grain level is reasonably well understood, the behaviour of a large assembly of these grains, with strongly non-linear interactions, demand concepts and methods that only recently emerged from the study of disordered systems in statistical mechanics. The main property of granular materials, that leads both to most of the non trivial phenomenology and to most of the theoretical difficulties, is the existence of a *large number of different microscopic metastable states* that are macroscopically equivalent. It turns out, quite interestingly, that this feature (metastability) is common to a wider class of materials in their 'jammed' state. This includes glasses, colloids, compressed emulsions and foams, spin-glasses, vortex glasses and other collectively pinned structures, etc.

There is a vast body of experimental results on granular materials that we do not aim to cover here (for reviews, see [81,80,56,57]). We will mainly restrict to *dry* grains in static and weakly driven situations. Correspondingly, we will focus on the statistical properties of the *static states* (and in particular the distribution of stresses) and on the glassy dynamics of *gently 'tapped' assemblies*, that slowly evolve from one static state to another. We have therefore excluded from these lectures, because of lack of time, 'strongly' driven situations, such as granular flows, avalanches and surface flows, dune formation, etc. This is not to suggest that these problems are less interesting and that collective effects are irrelevant. Quite on the contrary, the dynamics of strongly driven granular systems also displays remarkable effects, such as collisional clustering which generates non trivial spatial structures in granular flows, and invalidates simple hydrodynamical descriptions [72,96,16]. Some recent papers on these matters can be found in references [80,57,112,98,113].

Stress patterns in dry granular media exhibit some rather unusual features when compared to either liquids or elastic solids. For example, the vertical pressure below conical sand-piles does not follow the height of material above a particular point. Depending on the way the pile is prepared, it shows a *minimum* underneath the apex of the pile [128,29,140] when the pile is built from a point source, and a broad, flat maximum when it is built layer by layer from a uniform 'rain' of grains. Furthermore, local stress fluctuations are large, sometimes on length scales much larger than the grain size. For example, repeatedly pouring the very same amount of powder in a silo results in fluctuations of the weight supported by the bottom plate of 20% or more [30,141]. Weak perturbations of the packing can sometimes cause large rearrangements [44,50]. Qualitatively, these features are attributed to the presence of *stress paths* which can focus the stress field into localized regions and also deflect it to cause "arching" (see [49] for early qualitative experiments). More quantitative experiments were performed in [93,29,13], where the local fluctuations of the normal stress deep inside a silo or at the base of a sandpile were measured. It was found that the stress probability distribution is rather broad, decaying exponentially for large stresses. This behaviour was also found in numerical simulations [114], and more recently in other situations [109], such as compressed emulsions [31]. Similarly, standard 'triaxial'

test experiments used to determine the elastic properties of materials from the (macroscopic) relation between stresses and deformations show highly irreproducible, hysteretic behaviour which only seem to converge towards a well defined curve after a large number of deformation cycles have been imposed to the granular system in order to 'anneal' it down to a reproducible state.

The dynamics of slowly driven granular systems also exhibit unusual features when compared to either liquids or solids, and has actually much in common with *glasses*. In particular, the way these systems very slowly compact when vibrated, the unusual dependence of the density on the system history, etc. has strong similarities with the properties of glassy materials. At the phenomenological level, the dynamics of these systems appears to be a succession of hops between different (metastable) equilibrium states. The understanding of static and weakly driven granular assemblies therefore require a proper description of the statistical properties of these 'blocked' configurations. We now discuss these issues in the perspective of the present lectures. [1]

B. Theoretical issues

1. Static properties

How can one then describe the statics of granular materials on large length scales? The basic problem stems from the fact that the equilibrium equations for the stress tensor are not sufficient to determine the stress. For example, in two dimensions the stress tensor has three independent components, but there are only two equilibrium equations. Some additional assumptions about the properties of the material must be provided. For example, the assumption that the material is elastic and follows Hooke's law gives extra constraints on the stress tensor and allows one to solve the static problem as soon as some appropriate boundary conditions are given. For granular materials, the standard procedure is to use elastic or elasto-plastic theories from soil mechanics [148]. However, the relation between force chains on short length scales and an elasto-plastic description on large length scales is far from obvious. To our knowledge, no systematic procedure has ever been proposed to go from the mechanics at the grain level to coarse-grained equations that would justify the use of an elasto-plastic framework and estimate the parameters of the theory (effective elastic moduli, etc.). One of the main difficulty is that some indeterminacy exists already at the grain level, since many different configurations of the contact forces are allowed and satisfy local equilibrium. This leads to several conceptual problems: even if an elastic-like description of small perturbations around an arbitrary reference state (such as sound waves, for example) might make sense in general, the description of – say – a conical sandpile using elasto-plasticity theory [33] requires the identification of a (zero stress) reference state from which deformations can be defined, at least for *some* regions of the pile. In the case of a pile of infinitely hard grains (which should be the correct benchmark for an assembly of grains with a Young modulus much larger than the gravity induced stresses) that rests in one particular metastable state (among a large number of macroscopically equivalent ones), switching the gravity back to zero will hardly affect the packing. Each of these metastable states can thus equally well be taken as a reference state; on the other hand, it is precisely the stress pattern in one of these 'native' metastable state (i.e. obtained when grains come to rest without further tapping) that one wants to predict. One peculiarity of (dry) granular materials is the absence of tensile stresses between the grains; the cohesion of the assembly is therefore induced by the applied stress itself and the zero stress state is ill defined.

Even the description of small perturbations around a given reference state might be problematic. For example, the existence of a (large volume) limiting curve relating incremental stresses and deformations requires, as already mentioned above, at least some 'annealing' procedure to define a reproducible initial state. This limiting curve might not even exist in the absence of friction [44]. Even for moderate deformations, following the so-called consolidation phase, the response to cyclic loads in standard triaxial tests shows some significant irreversibility.

The absence of any obvious deformation field from which the stress tensor may be constructed has motivated an alternative, 'stress-only' approach [18,145,21,42]. The basic tenet of these theories is that in equilibrium, some (history dependent) large

---

[1] The content of these lecture notes owes a lot to my collaborators on these issues: Mike Cates, Philippe Claudin, Eric Clément, Dov Levine, Josh Socolar, Matthias Otto and Joachim Wittmer. Parts of these notes actually are extracted from various papers co-written with them. I have tried to add my own present understanding of the subject, in particular concerning Edwards ensembles, the hyperbolic approach to the statics of granular media, and their glassy dynamics, in particular dynamical heterogeneities. Some ideas are still speculative and are by no means intended to be definitive, but I hope that the theoretical concepts and methods are of sufficiently broad interest to deserve appearing in print in the present Les Houches volume. I wish to express my gratitude to Jean-Louis Barrat and Jorge Kurchan for giving me the opportunity of giving these lectures and for many very inspiring discussions. I thank the participants of the school for interesting comments and ideas, in particular G. Biroli, L. Berthier, E. Bertin, L. Cugliandolo, D. Fisher, A. Lefevre, J. Snoeijer, V. Viasnoff and O. White. I also thank E. Bertin for carefully reading the manuscript, and D. Bonamy, O. Dauchot, F. Daviaud, C. Godrèche, M. Mézard, J. N. Roux, R. da Silveira and E. Vincent for discussions.

scale relations between the components of the stress tensor should exist. These relations should be determined by the global statistical features of the particular metastable state in which the packing sits but not on its microscopic details, nor on the particular loading conditions, provided these do not lead to further rearrangements of the packing. Much as random collisions between molecules give rise, on large length scale, to well defined hydrodynamical equations, the hope is that an appropriate coarse-graining of the local force balance equations leads, on large length scales, to the missing 'closure' equation that allows to solve for the static equilibrium. (For rather formal attempts in this direction, see [62,2].) A well known relation of this type arises from the assumption that the material is everywhere on the verge of plastic failure, leading to a Mohr-Coulomb (non-linear) relation between the stress components [106], but we will motivate and discuss simpler relations below, based both on symmetry arguments [18] and on the consideration of simple rules for the transfer of stresses between adjacent grains [41]. The consequence of a fixed relation between the components of the stress tensor is that stresses obey an *hyperbolic* equation, as compared to the *elliptic* equations encountered in elasticity theory. This means that stresses 'propagate' or are 'transmitted' along lines: as discussed below, the characteristics of this hyperbolic equation are the mathematical transcription of the force chains that are well known to exist in granular materials [35].

2. Tapping and non thermal ensembles

As mentioned above, many different packings and configurations of the contact forces are compatible with the local equilibrium of each grain for a given macroscopic situation. This is actually intimately related to the fact that stresses in granular media often show large fluctuations; some kind of averaging is therefore needed to obtain reproducible results. In the case of sandpiles, one must repeat the construction of the pile several times, and use a pressure gauge that averages over a sufficiently large number of grains, in order to obtain a satisfactory stress profile that a statistical theory of blocked states should predict. Another possibility is to vibrate the packing such as to make it probe, during its evolution, several equilibrium states with the same macroscopic geometry. The natural question is then: with which statistical weight the different equilibrium (blocked) states appear in a given experiment? To what extent are these weights dependent on the dynamics that leads to the blocked states? Is the ensemble of 'native' (as-built) packings identical to the ensemble of packings obtained under tapping?

The simplest answer, proposed more than ten years ago by Sam Edwards, is to postulate that all blocked states with a given density are equiprobable [60]. This micro-canonical assumption defines what is now called the 'Edwards ensemble' [86]; it turns out that several toy models of jammed systems do obey, either exactly or to a good approximation, Edwards' prescription [5,52,127,45]. This is a first step towards a 'thermodynamical' description of out-of-equilibrium, dissipative systems [3,97,8,4]. However, several remarks of various nature should be made here.

- First, the analogy between tapping strength and temperature. In many cases, this is a useful intuitive guide and several experiments discussed in section X do indeed confirm the phenomenological analogies between the two. However, tapping is a long-wavelength excitation, whereas temperature in solid state physics is thought to give rise to very short wavelength fluctuations. Although the long-wavelength excitation probably cascades down, through collisions, to short wavelengths, ideas such as detailed balance and activated processes might be affected by the correlated nature of the noise. In this respect, the non trivial clustering patterns induced by the dissipative collisions might also obliterate simple ideas on the statistics of blocked states.
- One must distinguish at least two types of tapping excitations. One would be very gentle taps, that are insufficient to change the packing *geometry*, but do change the contact forces for each grain. In this case, tapping induces a random walk in 'force space', but for a fixed configuration of the grains. The Edwards hypothesis in this restricted case is to assign a uniform weight for all force configurations that (i) lead to static equilibrium (forces and torques on each grain add up to zero) and (ii) satisfy the Coulomb inequality at each contact. One can also drive the system with an amplitude such that the motion of grains is possible, in which case the dynamics is a random walk both in force space and in packing space. The extended Edwards ensemble in this case is to assign equal weight to any packing and any force configuration such that equilibrium is obeyed and the Coulomb inequality satisfied. In principle, the Edwards prescription could be correct in one case and not in the other, or in both, or in none, or more complicated situations still.
- The Edwards prescription is however ambiguous for continuous variables. In the 'gentle' tap case, one is tempted to interpret Edwards' measure as follows. Let us call $\vec{f}_i^{\alpha}$ the contact force on the α-th contact of the i-th grain, and $\vec{r}_i^{\alpha}$ the position of the contact point. We call μ the friction coefficient, and the indices N and T refer to the normal and tangential components of the force. The natural Edwards measure reads:

$$P\left(\{\vec{f}_i^{\alpha}\}\right) = \frac{1}{Z}\prod_i \left[\delta\left(\sum_\alpha \vec{f}_i^{\alpha}\right)\delta\left(\sum_\alpha \vec{f}_i^{\alpha}\times\vec{r}_i^{\alpha}\right)\prod_\alpha \Theta\left(\mu f_{i,N}^{\alpha} - |f_{i,T}^{\alpha}|\right)\right], \tag{1}$$

  which is a formal way to impose the constraints on each grain. (Θ is the step function). However, this assumes that the *a priori* measure on the forces is uniform, which is reasonable but not obvious. The usual microcanonical ensemble for particles is constructed similarly: one imposes the total energy of the system using a δ-function on an *a priori* uniform

measure on the canonical variables (position and momentum). However, in the latter case, this procedure is justified by the Liouville theorem which selects the relevant canonical variables. In general, however, there is an ambiguity since the assumption of uniformity is not invariant under changes of variables.

It is instructive to discuss the simplest case where the Edwards assumption can be discussed in details, and perhaps tested experimentally or numerically. Consider, as proposed by Ertas and Halsey, a single disk in a wedge [64]. In equilibrium, there are two contact points and therefore four unknowns: $f_{1,N}, f_{1,T}$ and $f_{2,N}, f_{2,T}$, where $f_{\alpha,T} > 0$ means that the force pushes upwards. These forces must lead to equilibrium, which gives three equations. There is therefore one degree of freedom which is not fixed by the equilibrium requirement, and is dynamically selected. It is easy to see that one must have $f_{1,T} = f_{2,T} = f_T$ and $f_{1,N} = f_{2,N} = f_N$. The Edwards measure then reads:

$$P(f_N, f_T) = \frac{1}{Z}\,\delta\left(f_N \sin\psi + f_T \cos\psi - \frac{1}{2}Mg\right)\Theta(\mu f_N - |f_T|), \tag{2}$$

where ψ is (half) the opening angle of the wedge. From this result, one can compute the distribution of the 'mobilization' ratio $r = f_T/f_N$, which is found to be parabolic:

$$P(r) \propto (\sin\psi + r\cos\psi)^2 \qquad (-\mu \le r \le \mu), \tag{3}$$

and, of course, zero outside the allowed interval $[-\mu, \mu]$. One could test this simple predictions by repeatedly tapping spheres made of different materials, and investigate the relevance of the tapping mode and the contact dynamics on the statistical ensemble of forces that one generates. This would be quite a valuable starting point, before speculating on more complex multi-grain situations. We will discuss below some numerical results that indeed suggest some dependence of the statistics of forces on the microscopic dynamics.

The Edwards prescription is in fact at the heart of the simplest 'scalar' model for the statistics of forces in granular materials, which was proposed in [93,46] to account for the empirical exponential tail in the distribution of forces. Although this model represents a highly stylized view of granular systems and cannot be expected to be accurate, it provides both an extremely rich theoretical benchmark and a pedagogical starting point for more elaborate descriptions.

II. THE SCALAR MODEL I: DISCRETE VERSION

A. Definition and motivation

The drastic simplification of the scalar model is to only retain one component of the stress tensor, namely the 'weight' $w = \sigma_{zz}$, and correspondingly, to only consider the force balance equation along the vertical axis. Again for simplicity, one can think that the grains reside on the nodes of a two-dimensional lattice, and are labeled by two integers: i in the horizontal direction and j in the vertical direction; j increases as one moves downwards. The equilibrium equation can then be written as:

$$w(i,j) = w_0 + q_+(i-1,j-1)w(i-1,j-1) + q_-(i+1,j-1)w(i+1,j-1) \tag{4}$$

where 'w_0' is the weight of each grain, and $q_\pm(i,j)$ are 'transmission' coefficients giving the fraction of weight which the (i,j) transmits to its right (resp. left) neighbour immediately below, such that $q_+(i,j) + q_-(i,j) = 1$ for all i,j's. The case of an ordered pile of identical grains and identical conditions for each contacts corresponds to $q_\pm = \frac{1}{2}$. In this case, the equation for the w's become identical to the Master equation describing the population of un-biased random walkers in a one space dimension (corresponding to i), evolving in 'time' (corresponding to j):

$$w(i,j) = w_0 + \frac{1}{2}\left[w(i-1,j-1) + w(i+1,j-1)\right]. \tag{5}$$

The term w_0 is a constant source of particles that are created uniformly in space and in time. We will explore this analogy further below.

Now, grain assemblies are usually not perfectly ordered: grains have various shapes and sizes; there are packing defects and irregularities; even for a perfectly ordered packing of identical grains one can expect that the history has imposed different contact loadings. In the above language, it means that the $q_\pm(i,j)$ are not all identical and reflect the above sources of randomness. The idea of Edwards, in this highly simplified framework, can easily be worked out, since each 'blocked' state corresponds to a particular choice of – say – $q_+(i,j)$ for all i,j. Provided $q_-(i,j) = 1 - q_+(i,j)$, equilibrium is ensured. The uniform measure on all blocked states, advocated by Edwards, merely translates, in the present case, as a uniform probability distribution for q_+ (or q_-) between 0 and 1. This defines the q model, which was originally written with an arbitrary number N of downward neighbours ($N = 2$ in the example above), and can thus be (in principle) generalized to three dimensions [93,46]. In this case, there are N coefficients q_α, $\alpha = 1, \cdots, N$ per grain, and the Edwards measure corresponds to the choosing all the q_α independently on each node i,j such that:

$$P(\{q_\alpha\}) = \frac{1}{Z}\delta\left(\sum_{\alpha=1}^{N} q_\alpha - 1\right). \tag{6}$$

Therefore, in the present case, Edwards prescription can be explicitly followed. It may seem *a priori* that this microcanonical assumption is too simple and can only lead to trivial predictions. However, as we discuss below, this is not the case: much as for gases where the microcanonical hypothesis can be used to derive, for example, the Maxwell distribution for the particle velocities, the q-model predicts a non trivial distribution for the local vertical stress.

B. Stress distribution and the exponential tail

The case of a uniform distribution of the q's is interesting because it leads to an exact solution for the local weight distribution $P(w)$ for large heights. Let us assume for the moment that the weights on neighbouring sites become asymptotically independent ([46,129]). Then $P(w)$ obeys the following mean-field equation:

$$P_{j+1}(w) = \int_0^1 dq_1 dq_2 \rho(q_1)\rho(q_2) \int_0^\infty dw_1 dw_2 P_j(w_1) P_j(w_2) \delta[w - (w_1 q_1 + w_2 q_2 + w_0)] \tag{7}$$

where $\rho(q)$ is the distribution of q, here taken to be $\rho(q) = 1$. In the limit $j \to \infty$, the stationary distribution P^* of this equation can be explicitly constructed and is given by:

$$P^*(w) = \frac{w}{\overline{w}^2} \exp -\frac{w}{\overline{w}} \tag{8}$$

where $2\overline{w} = jw_0$ is the average weight. For $N \neq 2$, the distribution is instead a Gamma distribution of parameter N; its small w behaviour is w^{N-1} while the large w tail is exponential. Liu et al. [93,46] have argued that this behaviour is generic and survives deviations away from the strict Edwards prescription: for example, the condition for the local weight w to be small is that all the N q's reaching this site are themselves small; the phase space volume for this is proportional to w^{N-1} if the distribution $\rho(q)$ is regular around $q = 0$. However, if instead $\rho(q) \propto q^{\gamma-1}$ when q is small, one expects $P^*(w)$ to behave for small w as $w^{-\alpha}$, with $\alpha = 1 - N\gamma < 0$.

Similarly, the exponential tail at large w is sensitive to the behaviour of $\rho(q)$ around $q = 1$. In particular, if the maximum value of q is $q_M < 1$, one can study the large w behaviour of $P^*(w)$ by taking the Laplace transform of equation (7). One finds in that case that $P^*(w)$ decays *faster* that an exponential:

$$\log P^*(w) \propto_{w\to\infty} -w^\beta \qquad \beta = \frac{\log N}{\log q_M N} \tag{9}$$

(Notice that $\beta = 1$ whenever $q_M = 1$, and that $\beta \to \infty$ when $q_M = 1/N$: this last case corresponds to an ordered lattice with no fluctuations). In this sense, the exponential tail of $P^*(w)$ is not universal: it requires the possibility that one of the q can be arbitrarily close to 1. This implies that all other q's originating from that point are close to zero, i.e. that there is a non zero probability that one grain is entirely bearing on one of its downward neighbours.

The success of the q-model with a uniform distribution of the q's is that it provides a simple explanation for the ubiquitous exponential tail for the distribution of forces, observed in many experimental and numerical situations. Note in particular that this exponential tail was observed in a regular packing of grains, suggesting that very strong heterogeneities in fact exist at the contact level. On the other hand, the probability to observe very small w is much underestimated by equation (8): see [29,114,13,41]. This might be due to the fact that *arching* effects are absent in this scalar model. A generalization of the q-model allowing for arching was suggested in [40], which dynamically generates some sites where $q_+ = 1$ and $q_- = 0$ (or vice versa). This indeed leads to much higher probability density for small weights. For a more detailed discussion of the relation between the q-model the experimental situations, in particular the role of boundaries, see [130].

C. The 'critical' case

There is however one special case of particular interest where the results for $P(w)$ are qualitatively different. Suppose that q is a random variable that only takes the values 0 or 1 with probability 1/2. This is called the Takayasu model, which is a model for directed river networks for example: at each site of the lattice a river flowing 'south-east' or 'south-west' is randomly deflected to the left or to the right. Rivers coalesce upon meeting. The 'source' term w_0 here describes a constant density of 'springs' that feed the river network. It can also be seen as a model of diffusing and aggregating clusters in a solution with a constant density of 'monomers' (that again play the role of the source term). In this case, it turns out [136] that the stationary distribution $P^*(w)$ becomes, for large heights, a power law, $P^*(w) \propto w^{-1-\mu}$, with $\mu = 1/3$ in dimension $d = 2$ (i.e. one 'spatial' and one 'temporal' dimension).

The exponent μ was derived analytically but can also understood as follows. Since the direction of the 'rivers' is, at each step, a random variable, the typical 'basin of attraction' of a given site is a parabolic object of height t and width $\sqrt{t}$. Therefore, on the order of $t^{3/2}$ 'springs' at most can contribute to the river flux on a given site; in other words, one expects the distribution $P^*(w)$ to take the scaling form:

$$P^*(w) = \frac{1}{w^{1+\mu}} F\left(\frac{w}{t^{3/2}}\right), \tag{10}$$

where F is a certain function which falls off fast for large arguments. On the other hand, since one must have $\langle w \rangle = w_0 t$ exactly, the exponent μ is fixed:

$$\int_0^{+\infty} dw\, w\, P^*(w) = w_0 t = t^{3\mu/2} \int_0^{+\infty} du\, \frac{F(u)}{u^\mu} \longrightarrow \mu = \frac{1}{3}. \tag{11}$$

(Note that the integral over u is convergent for this value of μ.)

Therefore, this model generates a power-law distribution for the local masses, and was proposed early on as a model of 'self-organized criticality'. In fact, the model is critical in the sense that any deviation of $\rho(q)$ from a sum of two equal delta peaks at 0 and 1 leads to an exponential truncation of $P^*(w)$ at large w's. Let us add several remarks:

- One can compute higher moments of the local weight, to find $\langle w^q \rangle \sim t^{3q/2-1/2}$ for $q > 1/3$. In particular, $\langle w^2 \rangle \sim t^{5/2}$, a result that we will recover below using direct method.
- One can also generalize the model to higher (spatial) dimensions, where one finds $\mu = 1/2$ for all $d \geq 3$ (with logarithmic corrections in $d = 3$).
- Consider a rectangular sample of width W and height H. What is the order of magnitude of the largest weight encountered at the bottom ? For a pure power law distribution such as Eq. (10) with $t \to \infty$, the maximum value of w is known to be of order $w_{\max} \sim W^{1/\mu}$. This estimate can obviously only be valid if $w_{\max}$ is found to be much smaller than the truncation imposed by the function F, which is of order $H^{3/2}$. This requires $W \ll H^{3\mu/2} \sim H^{1/2}$. However, in this regime where W is smaller than the diffusion length, the very argument leading to Eq. (10) breaks down, since the maximum weight now scales like WH, and not as $H^{3/2}$. Extending the argument, we now find that the distribution of weights reads:

$$P^*(w) = \frac{1}{Ww} G\left(\frac{w}{WH}\right), \qquad (W \ll aH^{1/2}). \tag{12}$$

  Therefore, (a) for $W \gg H^{1/2}$, the maximum value of w is imposed by the cut-off and of order $H^{3/2}$, and not N^3. Correspondingly, the participation ratio $Y_2 = \sum_{i=1} w_i^2/(w_0 HW)^2$ that characterizes the 'localization' of the weight is of order $H^{1/2}/W \ll 1$. In the case (b) $W \ll H^{1/2}$, on the other hand, the weight is localized on a finite number of sites, and $Y_2 \sim 1$.

III. THE SCALAR MODEL II: CONTINUOUS LIMIT AND PERTURBATION THEORY

A. Continuous limit of the scalar model

Let us focus on the case $N = 2$ and define v to be such that $q_\pm(i,j) = (1 \pm v(i,j))/2$. If v is small, the local weight is smoothly varying, and the discrete equation (4) can then be written in the following differential form:

$$\partial_t w + \partial_x (vw) = \rho + D_0 \partial_{xx} w \tag{13}$$

where $x = ia$ and $t = j\tau$ are the horizontal and (downwards) vertical variables corresponding to indices i and j, and a and τ are of the order of the size of the grains. The vertical coordinate has been called t for its obvious analogy with time in a diffusion problem. ρ is the density of the material (the gravity g is taken to be equal to 1), and D_0 a 'diffusion' constant, which depends on the geometry of the lattice on which the discrete model has been defined. This diffusion constant is of the order of magnitude of the size of the grains, a.

In this model and in the following, we shall assume that the density ρ is not fluctuating. Density fluctuations could be easily included; it is however easy to understand that the resulting relative fluctuations of the weight at the bottom of the pile decrease with the height of the pile H as $H^{-1/2}$, and are thus much smaller than those induced by the randomly fluctuating direction of propagation, encoded by q (or v), which remain of order 1 as $H \to \infty$.

Two interesting quantities to compute are the average 'response' $G(x,t|x_0,t_0)$ to a small density change at point (x_0,t_0), measured at point (x,t), and the correlation function of the force field, $C(x,t,x',t') = \langle w(x,t) w(x',t') \rangle_c$, where the averaging is taken over the realizations of the noise $v(x,t)$.

Equation (13) shows that the scalar model of stress propagation is identical to that describing tracer diffusion in a (time dependent) flow $v(x,t)$. This problem has been the subject of many recent works in the context of turbulence [38]; interesting

qualitative analogies with that field can be made. In particular, 'intermittent' bunching of the tracer field correspond in the present context to patches of large stresses, which may induce anomalous scaling for higher moments of the stress field correlation function.

• Fourier transforms.

The limit where $a \to 0$ is ill defined and leads to a divergence of the perturbation theory for large wave-vectors k. We thus choose to regularize the problem by working within the first Brillouin zone, i.e., we keep all wave vector components within the interval $\mathcal{I} = [-\Lambda, +\Lambda]$, where $\Lambda = \frac{\pi}{a}$. Our Fourier conventions for a given quantity f will then be the following:

$$f(x,t) = \int_{-\Lambda}^{\Lambda} \frac{dk}{2\pi} e^{\imath kx} f(k,t) \tag{14}$$

$$f(k,t) = \ell_x \sum_{x=-\infty}^{+\infty} e^{-\imath kx} f(x,t) \tag{15}$$

One has to be particularly careful when computing convolution integrals, such as $\int \frac{dq}{2\pi} f_1(q) f_2(k-q)$ which must be understood with limits $-\Lambda + k, \Lambda$ (resp. $-\Lambda, \Lambda + k$) if $k \geq 0$ (resp. $k \leq 0$). An important example, which will appear in the response function calculations, is:

$$\int_{q, k-q \in \mathcal{I}} \frac{dq}{2\pi} q = \frac{\Lambda k}{2\pi} + \mathcal{O}(k^2) \tag{16}$$

Let us then take the Fourier transform of equation (13) along x, to obtain:

$$(\partial_t + D_0 k^2) w_k = \rho_k + \imath k \int \frac{dq}{2\pi} w_q v_{k-q} \tag{17}$$

Our aim is to calculate, in the small-k limit, the average response (or Green) function $G(k, t-t')$ defined as the expectation value of the functional derivative $\langle \delta w(k,t)/\delta \rho(k,t') \rangle$; and the two points correlation function of w, $C(k,t) = \langle w(k,t) w(-k,t) \rangle$.

• The noiseless Green function.

The noiseless (bare) Green function (or 'propagator') G_0 is the solution of the equation where the 'velocity' components v_q are identically zero: $(\partial_t + D_0 k^2) G_0(k, t-t') = \delta(t-t')$ which is:

$$G_0(k, t-t') = \theta(t-t') e^{-D_0 k^2 (t-t')} \tag{18}$$

In real space, the propagator is simply the heat kernel,

$$G_0(x, t-t') = \frac{\theta(t-t')}{\sqrt{4\pi D_0 (t-t')}} e^{-\frac{x^2}{4D_0(t-t')}}. \tag{19}$$

This shows that in the non-disordered scalar model, the stress 'diffuses', as already noticed above in the discrete formulation of the model, see Eq. (5).

• Statistics of the noise $v(x,t)$.

The noise term v represents the effect of local heterogeneities in the granular packing. The mean value of the noise v is taken to be zero, and its correlation function is chosen for simplicity to be of the factorable form $\langle v(x,t) v(x',t') \rangle = \sigma^2 g_x(x-x') g_t(t-t')$, where g_x and g_t are noise correlation functions along x and t axis. We shall take g_x and g_t to be short-ranged (although this may not be justified: fluctuations in the micro-structure of granular media may turn out to be long-ranged due to e.g. the presence of long stress paths or arches), with correlation lengths ℓ_x and ℓ_t. Our aim is to describe the system at a scale L much larger than both the lattice and the correlation lengths: a, τ, ℓ_x, $\ell_t \ll L$. This will allow us to look for solutions in the regime $k, E \to 0$, where k and E are the conjugate variables for x and t respectively, in Fourier-Laplace space. However, we shall see below that the limit $a, \tau, \ell_x, \ell_t \to 0$ can be tricky, and must be treated with care: this is because the noise appears in a multiplicative manner in equation (13). For computational purposes, we shall often implicitly assume that the probability distribution of v is Gaussian; this might however introduce artifacts which we try to discuss.

• Ambiguities due to multiplicative noise. Ito vs. Stratonovitch.

In equation (17), we have omitted to specify the dependence on the variable t. There is actually an ambiguity in the product term $w_q v_{k-q}$. In the discrete q-model model [93], the $q_\pm$'s emitted from a given site are independent of the value of the weight on that site. In the continuum limit, this corresponds to choosing $w_q(t)$ to be independent of $v_{k-q}(t)$, or else that the v's must be thought of as slightly posterior to the w's (i.e the product is read as $w_q(t-0)v_{k-q}(t+0)$). In this case, the average of equation (17) is trivial and coincides with the noiseless limit; hence $G = G_0$. This can be understood directly on the discrete model by noticing that the Green function $G(i,j|0,0)$ can be expressed as a sum over paths, all starting at site $(0,0)$, and ending at site (i,j):

$$G(i,j|0,0) = \sum_{\text{paths } \mathcal{P}} \prod_{(k,l)\in\mathcal{P}} q_\pm(k,l) \tag{20}$$

where the $q_\pm(k,l)$ are either $q_+(k,l)$ or $q_-(k,l)$, depending on the path. Since each bond $q_\pm(k,l)$ appears only once in the product, the averaging over q is trivial and leads to:

$$G(i,j|0,0) = \sum_{\text{paths } \mathcal{P}} 2^{-j} \equiv G_0(i,j|0,0) \tag{21}$$

(Note that this argument fails for the computation of the correlation function C, since paths can 'interfere'. We shall return later to this calculation.)

The above choice corresponds to Ito's prescription in stochastic calculus. Another choice (i.e. Stratonovitch's prescription) is however possible, which corresponds to the proper continuum time limit in the case where the correlation length ℓ_t is very small, but not smaller than a. In this case, the w's and the v's cannot be taken to be independent. This is the choice that we shall make in the following.

B. Calculation of the averaged response and correlation functions.

Two approaches will be presented. The first one, based on Novikov's theorem, leads to exact differential equations for G and C, which can be fully solved. The second one is a mode-coupling approximation (MCA), based on a re-summation of perturbation theory. It happens that, for this particular model where the noise is Gaussian and short range correlated in time, both approaches give the same results, because perturbation theory is trivial. In other cases, though, where exact solutions are no longer available, the MCA is in general very useful to obtain non perturbative results.

We shall see that the effect of the noise is to widen the diffusion peak: D_0 is renormalized by an additional term proportional to the variance of the noise v.

• Novikov's theorem. Exact equations for G.

Novikov's theorem provides the following identity, valid if the v are Gaussian random variables:

$$\Big\langle w(k,t)v(k',t)\Big\rangle = \int_0^t dt' \int dq \left\langle \frac{\delta w(k,t)}{\delta v(q,t')} \right\rangle \Big\langle v(q,t')v(k',t)\Big\rangle \tag{22}$$

Such a term actually appears in equation (17), after transformation into an equation for G:

$$(\partial_t + D_0 k^2) G(k,t-t') = \delta(t-t') - \imath k \frac{\delta}{\delta\rho(k,t')} \int \frac{dq}{2\pi} \langle v(q,t) w(k-q,t)\rangle \tag{23}$$

In the limit where $\ell_x = a \to 0$, the noise correlation is of the form: $\langle v(q,t)v(q',t')\rangle = 2\pi\sigma^2\delta(q+q')g_t(t-t')$, with g_t peaked in $t=t'$ such that $f(t')g_t(t-t') \simeq f(t)g_t(t-t')$ for any function f. From formally integrating equation (17) between t' and t, one can express the equal-time derivative $\delta w/\delta v$ as:

$$\left.\frac{\delta w(k,t)}{\delta v(k',t')}\right|_{t'=t-0} = -\imath k w(k-k',t) \tag{24}$$

and thus obtain:

$$(\partial_t + D_0 k^2) G(k,t-t') = \delta(t-t') - 2\pi\sigma^2 k G(k,t-t') \int_0^t dt' g_t(t-t') \int \frac{dq}{2\pi}(k-q) \tag{25}$$

Using the shape of the function g_t, the first integral is $1/2$. The second one is a convolution integral, and its value is $\Lambda k/2\pi + \mathcal{O}(k^2)$ (see equation (16)). The final differential equation for G is then, in the small-k limit, a diffusion equation with a renormalized diffusion constant:

$$D_R = D_0 + \frac{\sigma^2 \Lambda}{2} \tag{26}$$

It is interesting to note that the model remains well defined in the limit where the 'bare' diffusion constant is zero, since a non zero diffusion constant is induced by the fluctuating velocity v. This would not be true if Eq. (13) was interpreted with the Ito convention, where the fluctuating velocity would *not* lead to any spreading of the average density.

The most important conclusion is thus that, in the present scalar model, stresses propagates essentially vertically, even in the presence of disorder: taking $\ell \sim a$ (where $\ell_x \sim \ell_t \sim \ell$), the response at depth H to a small perturbation is confined within a distance $\propto \sqrt{D_R H}$ from the vertical. Since $D_R \simeq \ell^2/a$, $\sqrt{D_R H}$ is much less than H in the limit where $H \gg \ell^2/a$, i.e. when the height of the assembly of grains is much larger than the grain size.

- Exact equations for C.

Exact equations can also be derived for C, following very similar calculations. From equation (17), one can deduce the corresponding one for $w(k,t)w(-k,t)$. Upon averaging, Novikov's theorem has to be used on quantities such as $\langle w(k,t)v(q,t)w(-k-q,t)\rangle$, finally leading to:

$$(\partial_t + 2D_R k^2) C(k,t) = \hat{\sigma}^2 k^2 \left[\int \frac{dq}{2\pi} C(q,t) + \rho^2 t^2 \right], \tag{27}$$

where $\hat{\sigma}^2 = (2\pi)\sigma^2$. Going to Laplace transforms in time leads to:

$$(E + 2D_R k^2) C(k,E) - C(k,t=0) = \hat{\sigma}^2 k^2 \left[\tilde{C}(E) + 2\rho^2 E^{-3} \right] \tag{28}$$

where $\tilde{C}(E) = \int \frac{dk}{2\pi} C(k,E) \equiv \int dt\, e^{-Et} C(x=0,t)$. This allows one to get a closed equation on $\tilde{C}(E)$:

$$\tilde{C}(E) = \int \frac{dk}{2\pi} \frac{C(k,t=0)}{E + 2D_R k^2} + \int \frac{dk}{2\pi} \frac{\hat{\sigma}^2 k^2}{E + 2D_R k^2} \left(\tilde{C}(E) + 2\rho^2 E^{-3} \right). \tag{29}$$

In the limit where $E \to 0$, the first term on the right hand side is of order $E^{-1/2}$, whereas the coefficient of $\tilde{C}(E)$ is equal to $\hat{\sigma}^2/2D_R$. This shows that one has to distinguish two cases:

- $\hat{\sigma}^2 < 2D_R$. This corresponds, for the discrete model, to the generic case where $\rho(q)$ is not the sum of two delta peaks at $q=0$ and $q=1$. The equation for $\tilde{C}(E)$ becomes, for $E \to 0$:

$$\left(1 - \frac{\hat{\sigma}^2}{2D_R} \right) \tilde{C}(E) \approx \frac{\hat{\sigma}^2}{2D_R} 2\rho^2 E^{-3}, \tag{30}$$

  or $\tilde{C}(E) \sim E^{-3}$. Transforming back to real times leads to $C(x=0,t) \sim t^2$, which is consistent with the results obtained within the discrete scalar model, where the local weight is of order t, with relative fluctuations of order one. Once one knows $C(x=0,t)$, one can obtain, from Eq. (27), the full function $C(x,t)$. When $x \gg a$, one finds:

$$C(x,t) = t^{3/2} \mathcal{C}\left(\frac{x}{\sqrt{t}} \right), \tag{31}$$

  where $\mathcal{C}(.)$ is a scaling function computed explicitly in [115]. This results shows (i) that the correlations extend over distances $\sqrt{t}$, as expected from the diffusive nature of the model, and (ii) that $C(x \neq 0, t) \ll C(x=0)$, meaning that asymptotically correlations between different sites vanish. The assumption that different sites become independent (which is a stronger statement) was already used above to obtain the Gamma distribution of the local weights in the scalar model. We see that this assumption is at least consistent.

- $\hat{\sigma}^2 = 2D_R$. This corresponds exactly, as shown in [115] to the critical Takayasu model where q can only take the values 0 and 1 with equal probability. In this case, a more careful analysis of the limit $E \to 0$ must be performed. Using the fact that:

$$\int \frac{dk}{2\pi} \frac{2D_R k^2}{E + 2D_R k^2} = 1 - E \int \frac{dk}{2\pi} \frac{1}{E + 2D_R k^2} \sim 1 - \sqrt{E/8D_R}, \tag{32}$$

  we now find that $\tilde{C}(E) \sim E^{-7/2}$, or $C(x=0,t) \sim t^{5/2}$. Again, this is consistent with the direct scaling analysis presented above. Extending the analysis to $x \neq 0$ now leads to:

$$C(x \neq 0, t) = t^2 \mathcal{C}_c\left(\frac{x}{\sqrt{t}} \right), \tag{33}$$

  where the critical scaling function $\mathcal{C}_c(.)$ can also be computed explicitly [115], and is different from $\mathcal{C}(.)$. Note that the asymptotic de-correlation of different sites still takes place, since $C(x \neq 0, t) \ll C(x=0,t)$.

• Perturbation theory.

The above method gives exact results, essentially because $v(x,t)$ is short range correlated in time: $\delta w/\delta v$ is then only needed at coinciding times, where it is known, and equal to 1. This would not be true in general; furthermore Novikov's theorem requires v to be Gaussian. It is thus interesting to show how a systematic perturbation scheme can be made to work by the use of diagrams to represent equation (17). The MCA (Mode Coupling Approximation) is then a particular re-summation scheme of this set of diagrams, which was discussed in detail in [19], which sometimes provide interesting non perturbative results.

Equation (17) is multiplied on the left by the operator G_0 (see equation (18)), and then re-expressed as follows:

$$w(k,t) = G_0(k,t) \otimes \rho(k,t) - \imath k G_0(k,t) \otimes \int \frac{dq}{2\pi} w(q,t) v(k-q,t) \tag{34}$$

$\otimes$ meaning a t-convolution product. This equation can be represented with diagrams as follows: as shown in figure 1, we represent the source ρ by a cross, the 'bare' propagator G_0 by a plain line and the noise v by a dashed line. The first term of

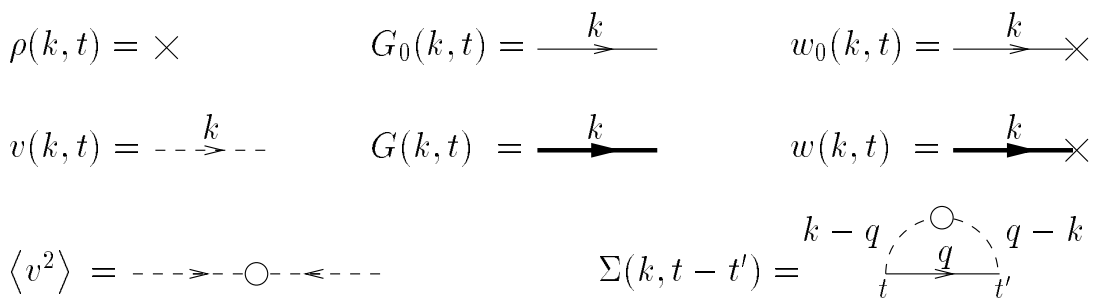

FIG. 1. definition of various diagrams.

equation (34), which is the noiseless solution w_0, is then obtained as the juxtaposition of a plain line and a cross. The arrow flows against time (i.e it is directed from t to $t' < t$). The juxtaposition of two objects means a t-convolution product. By definition w is represented by the juxtaposition of a bold line and a cross (this is consistent with the identification of a bold line with the full propagator G). The diagrammatic version of equation (34) is then:

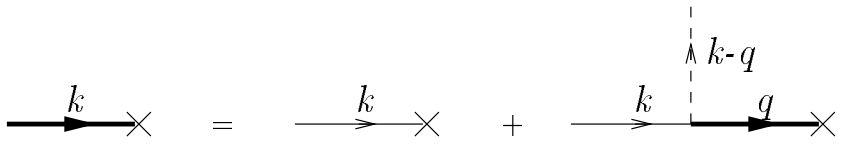

(35)

The 'vertex' stands for $-\imath k \int \frac{dq}{2\pi}$, the two emerging wave vectors being q and $k-q$ (node law). One can now iterate this equation. To second order, one obtains:

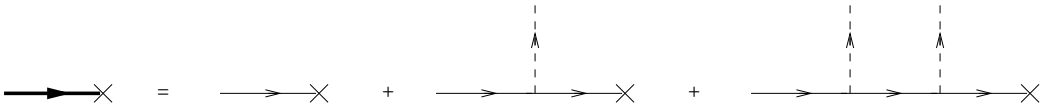

(36)

The corresponding equation for G is obtained by taking the derivative $\delta/\delta\rho$, and averaging over the noise v. Since $\langle v \rangle = 0$, the second diagram vanishes. We represent the noise correlator by a dashed line with a centered circle (see figure 1), and obtain:

(37)

or $G = G_0 + G_0 \Sigma G_0$, where Σ is called the self-energy (see figure 1). Actually, one can re-sum exactly all the diagrams corresponding to $G_0\Sigma G_0$, $G_0\Sigma G_0\Sigma G_0$ to obtain the Dyson equation $G = G_0 + G_0\Sigma G$.

The MCA amounts to replacing the 'bare' propagator in the diagram for Σ by the full propagator G. (Note that the MCA is of course exact to second order in perturbation theory). We then obtain a self-consistent equation for G:

$$\Sigma_{\text{MCA}} = G_0^{-1} - G_{\text{MCA}}^{-1} =$$

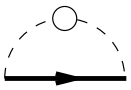

(38)

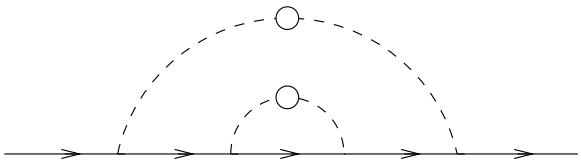

FIG. 2. Example of a diagram included in the MCA. Note that this diagram is zero if the noise is δ-correlated in time.

Diagrams like the one drawn in figure 2 are now also included. The self-energy Σ_{MCA} can be easily computed, we get

$$\Sigma_{\text{MCA}}(k, t-t') = -2\pi\sigma^2 k \int \frac{dq}{2\pi} q G_{\text{MCA}}(q, t-t') g_t(t-t') \tag{39}$$

In the special case where g_t is peaked around $t = t'$, we can make the approximation $G(q, t-t')g_t(t-t') \simeq G(q,0)g_t(t-t') = g_t(t-t')$ (since by definition $G(q,0) = 1$). We thus get, using equation (16)), $\Sigma_{\text{MCA}}(k, t-t') = -\sigma^2\Lambda k^2 g_t(t-t')$. The expression for G^{-1}_{MCA} is thus identical to the one obtained with the exact approach, as can be seen by comparing equation (25) and $G_0^{-1}G = 1 + \Sigma G$.

Note that one can also calculate the influence of a non zero skewness ς, or kurtosis κ, which are the normalized third and fourth cumulant of the noise v. In this case, three and four dashed lines (corresponding to v) can be merged, leading to a contribution to D, of the order of $\varsigma\sigma^3$ or $\kappa\sigma^4$.

Let us turn now to the calculation of the correlation function $C(k,t) = \langle w(k,t)w(-k,t)\rangle$. The basic object which corresponds to the self-energy is now the 'renormalized source' spectrum $S(k,t,t')$ defined as: $C = G \otimes S \otimes G$. S is drawn as a filled square. S_0 (empty square) is the correlation function source term which encodes the initial conditions (see below). The two first terms of the expansion are

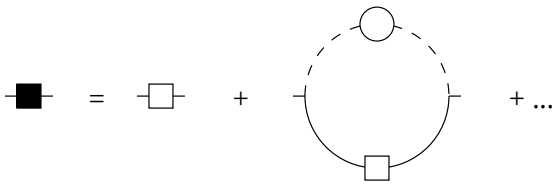

(40)

Here again, we transform the perturbative expansion into a closed self-consistent equation for S by replacing G_0 and S_0 in (40) by G and S respectively. The final equation for C reads:

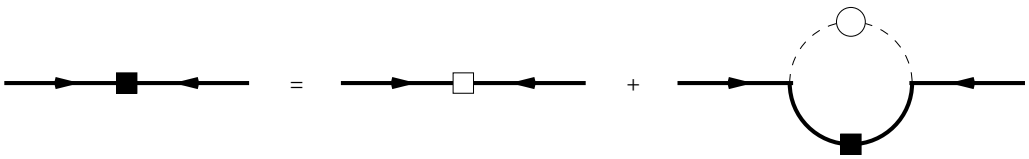

(41)

or, written explicitly,

$$\begin{aligned} C(k,t) = &\int_0^t dt' \int_0^t dt'' G(k, t-t') S_0(k, t', t'') G(-k, t-t'') + \\ &\hat{\sigma}^2 k^2 \int_0^t dt' \int_0^t dt'' G(k, t-t') \int \frac{dq}{2\pi} C(q, t', t'') g_t(t'-t'') G(-k, t-t'') \end{aligned} \tag{42}$$

If we choose the source term to be an overload localized at $t = 0$, we get: $S_0 = \langle \rho(k,t')\rho(-k,t'')\rangle = C(k,0)\delta(t')\delta(t'')$.

Using the fact that g_t is peaked around $t' = t''$, we again recover exactly the equation (27) above, showing again that MCA is exact in this special case.

C. Further results: the un-averaged response function

The *average* Green function described above is thus a Gaussian of zero mean, and of width growing as $\sqrt{D_R t}$. However, for a *given* environment, the Green function is not Gaussian, presenting sample dependent peaks (see Figure 3). Note however that, contrarily to what we shall find below for the tensorial case, the un-averaged Green function remains everywhere positive. Furthermore, the quantity $[x](t)$, defined as the displacement of the centroid of the weight distribution beneath a point source

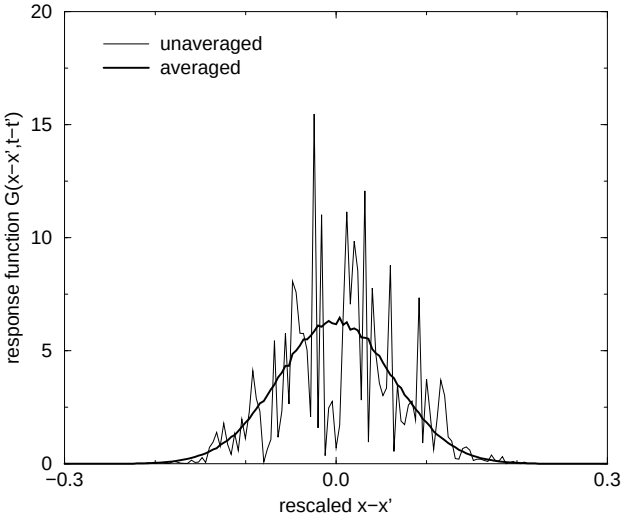

FIG. 3. Averaged (bold line) and un-averaged (thin line) response function of the scalar model, obtained numerically by simulating the q-model. One can notice how 'non self averaging' is the response function, i.e. how different it is for a given environment as compared to the average. Note also that the un-averaged Green function is everywhere positive.

in a given realization:

$$[x](t) = \int_{-\infty}^{+\infty} dx' \; x' \; \frac{\delta w(x',t)}{\delta \rho(0,0)} \tag{43}$$

typically grows with t. More precisely, one can show that:

$$\langle [x](t) \rangle = 0 \quad \text{but} \quad \left\langle [x]^2(t) \right\rangle \propto t^{1/2} \tag{44}$$

meaning that the 'center' of the Green function wanders away from the origin in a sub-diffusive fashion, as $t^{1/4}$. This behaviour has actually been obtained in another context, that of a quantum particle interacting with a time dependent random environment. Physically, the q-model can indeed be seen as a collection of time dependent scatterers, converting in-going waves into outgoing waves with certain partition factors $q_+, q_- = 1 - q_+$, a problem equivalent to the one dimensional Schroedinger equation with a time dependent random potential (see the discussion in [122,47]). In two dimensions (plus time), the wandering of the packet center $[x](t)$ is only logarithmic (and disappears in higher dimensions [47]).

Similarly, the participation ratio $Y_2 = \int dx \left\langle w^2(x,t) \right\rangle$ can be computed, and is found to be $\sim t^{-1/2}$, which means that the weight is not localized on a finite number of sites in this model when $t \to \infty$.

D. The scalar model with bias: Edwards' picture of arches

Up to now, we have considered the mean value of v to be zero, which reflects the fact that there is no preferred direction for stress propagation. In some cases however, this may not be true. Consider for example a sandpile built from a point source: the history of the grains will certainly in-print a certain oriented 'texture' to the contact network, which can be modeled, within the present scalar model, as a non zero value of $\langle v \rangle$, the sign of which depends on which side of the pile is chosen. In other words, the isotropic Edwards assumption for the local stress transmission is expected to break down when the history of the packing explicitly breaks a symmetry.

Let us call V_0 the average value of v on the $x \geq 0$ side of the pile, and $-V_0$ on the other side. The differential equation describing propagation now reads, in the absence of disorder:

$$\partial_t w + \partial_x \left[V_0 \; \mathrm{sign}(x) w \right] = \rho + D_0 \partial_{xx} w \tag{45}$$

For a constant density $\rho = \rho_0$, and for $D_0 = 0$, the weight distribution is then the following:

$$w(x,t) = \frac{\rho_0 x}{V_0} \qquad \text{for } 0 \le x \le V_0 t$$
$$w(x,t) = \frac{\rho_0 (ct-x)}{c-V_0} \qquad \text{for } V_0 t \le x \le ct \tag{46}$$

where $c = 1/\tan\phi$ (ϕ is the angle made by the slope of the pile with the horizontal x axis). For $D_0 \neq 0$, the above solution is smoothed. In any case, the local weight reaches a *minimum* around $x = 0$. Equation (45) gives a precise mathematical content to Edwards' model of arching in sand-piles [59], as the physical mechanism leading to a 'dip' in the pressure distribution [128]. As discussed elsewhere [145,146], this can be taken much further within a tensorial framework (see Section V A).

Equation (45) with noise can in fact be obtained naturally within an extended q-model, with an extra rule accounting for the fact that a grain can slide and lose contact with one of its two downward neighbour when the shear stress is too large [40]. This generically leads to arching; in the sandpile geometry and for above a certain probability of (local) sliding, the effective 'velocity' V_0 becomes non zero and the weight profile (46) is recovered [40]. However, this extra sliding rule implicitly refers to the existence of shear stresses, which are absent in the scalar model, but which are crucial to obtain symmetry breaking effects modeled by a non zero V_0 (see also the discussion in section V A. It is thus important to consider from the start the fact that stress has a tensorial, rather than scalar, nature. This is what we investigate in the following sections.

IV. STATIC INDETERMINACY; ELASTICITY AND ISOSTATICITY

A. Elasticity and response functions

As mentioned in the introduction, the sole equilibrium equations are not sufficient to determine the stress tensor of an arbitrary material. In $d = 2$, one has two equations and three independent components of the stress tensor. In $d = 3$, there are three equations for six independent components of σ_{ij}. In elastic materials, this indeterminacy is lifted when one adds the constraint that the stress tensor is linearly related to the strain. The most general linear relation between stresses and strains is given by:

$$\sigma_{ij} = \lambda_{ijkl} u_{kl} \tag{47}$$

where σ_{ij} denotes the components of the stress tensor, u_i is the displacement field, $u_{ij} = \frac{1}{2}(\partial_j u_i + \partial_i u_j)$ those of the strain tensor, and summation over repeated indices is implied. The four index tensor λ_{ijkl} satisfies certain symmetry conditions [89].

In order to close the problem for the stress tensor, one imposes a condition of 'compatibility', which in $d = 2$ reads:

$$\partial_z^2 u_{xx} + \partial_x^2 u_{zz} - 2\partial_x \partial_z u_{xz} = 0, \tag{48}$$

resulting simply from the fact that the tensor u_{ij} is built with the derivatives of a vector u_i. This is enough to find a closed equation for the stresses (in $d = 2$) [110]:

$$\left(\partial_z^4 + t\partial_x^4 + 2r\partial_x^2\partial_z^2\right)\sigma_{ij} = 0 \tag{49}$$

where the two independent coefficients t and r can be expressed in terms of the components of λ_{ijkl}. *Isotropic* elasticity corresponds to $r = t = 1$.

Expanding the stresses in Fourier modes, it is easy to see that the solutions of the equations (49) are of the form

$$\sigma_{tt} = \int_{-\infty}^{+\infty} \mathrm{d}q \sum_k a_k(q)\, e^{iqx + iX_k qz}, \tag{50}$$
$$\sigma_{xt} = C_{xz} - \int_{-\infty}^{+\infty} \mathrm{d}q \sum_k a_k(q)\, X_k\, e^{iqx + iX_k qz}, \tag{51}$$
$$\sigma_{xx} = C_{xx} + \int_{-\infty}^{+\infty} \mathrm{d}q \sum_k a_k(q)\, X_k^2\, e^{iqx + iX_k qz}, \tag{52}$$

where C_{xx} and C_{xz} are constants. From equation (49) we see that the X_k are the roots of the following quartic equation

$$X^4 + 2rX^2 + t = 0, \tag{53}$$

which has four solutions:

$$X = \pm\sqrt{-r \pm \sqrt{r^2 - t}}. \tag{54}$$

Hence the index k runs from 1 to 4. The four functions $a_k(q)$ and the constants C_{xx} and C_{xz} must be determined by the boundary conditions. A particularly interesting boundary condition is when one imposes a localized force at the top surface of

the material. The shape of the stress *response function* to such a localized force will be of central importance in the following discussion. One can establish the existence of various 'phases' in the r, t plane in terms of the shape of the response function, as obtained from the calculations presented in [110]. In that plane, the line $t = r^2$, for $r < 0$, separates the so called *hyperbolic* and the *elliptic* regions. For $t > r^2$, the above roots X_k are complex whereas for $t < r^2$ and $r > 0$ the roots X_k are purely imaginary. These two regions correspond to the *elliptic* regime, which is in fact the only accessible one in the context of classical elasticity where the coefficients r and t are constrained by the fact that the undeformed state is a minimum of the elastic energy. As shown in details in [110], the response function has a unique, broad peak of width growing linearly with depth in the region $t < r^2$ and $r > 0$, whereas the response function becomes *double peaked* in the region $r < 0$, $t > r^2$ (with a width again scaling linearly with depth). As one approaches the line $t = r^2$, the two peaks become narrower and narrower before becoming two delta-function peaks exactly on the transition line. At this point and below the transition, the system is *hyperbolic*; this limit behaviour will actually emerge naturally below in the context of granular materials.

B. Indeterminacy at the grain level and isostaticity

Elasticity theory can also be seen as the long-wavelength description of a network of beads and springs, for which the local equilibrium equations are fully determined at each node. When the network is disordered, the theoretical difficulty is to compute the effective elastic constants in terms of the probability distribution and correlations of the microscopic springs. The same problem arises when one wants to compute the effective conductivity, or the effective permittivity, etc. of a composite material. But in all these problems, the *microscopic* equations are sufficient to solve the problem in principle.

For an assembly of grains, this is not the case. The indeterminacy of the static equilibrium exists already at the grain level (see the simple case discussed in section I B 2). In principle, one should describe in details the microscopic history of each contact in order to determine the precise configuration of forces within a given packing. There are however special cases where this is not the case, and where all contact forces are fully determined by the packing geometry. These situations are called isostatic, and play a special role. These equilibria are in some sense critical since the opening of one contact necessarily leads to some rearrangements. Some arguments have been put forward to suggest that an assembly of grains relaxing towards static equilibrium will most probably stop *as soon as they are stable*, i.e., in one of these isostatic states [14]. A similar statement is actually *exact* in the context of mean-field spin-glasses, where the equilibrium states reached dynamically are marginally stable, in the sense that the spectrum of the eigenvalues λ of the Hessian (matrix of second derivatives of the energy) vanishes precisely at $\lambda = 0$. Before discussing the validity of the idea that these marginal states play a special role in granular media, let us first discuss the geometrical conditions necessary for isostaticity [125].

Consider *frictionless* grains in two dimensions. There are, per grain, two equilibrium equations since the torque is automatically zero, and one (normal) force per contact that must be determined. If N is the total number of grains and N_c the total number of contacts, the number of unknowns is N_c and the number of equations in $2N$. Therefore, one can (generically) find static solutions only if $N_c \geq 2N$. Since each contact concerns two grains, the average number of contact per grain is $n_c = 2N_c/N$ and the condition for the existence of solutions is $n_c \geq 4$. The marginal case is when $n_c = 4$, where the number of unknowns is equal to the number of equations, and corresponds to the isostatic case. The hyper-static case corresponds to a strict inequality. If the friction coefficient is non zero, then the zero-torque condition provides a third equation for each grain. If we call φ the fraction of contacts where friction is fully mobilized (i.e. such that $|F_T| = \mu F_N$), one has $\varphi \cdot N_c + (1-\varphi) \cdot 2N_c$ unknowns (one per mobilized contact, two for un-mobilized contacts). The stability condition now reads $n_c(1 - \varphi/2) \geq 3$. (Note that the frictionless case corresponds to $\varphi = 1$). In three dimensions, the same argument leads to $(3 - \varphi)n_c \geq 12$, the isostatic case corresponding to an equality. The corresponding 'stability' diagram is shown in Fig. 4.

C. Numerical simulations and Edwards' assumption

So, are three dimensional packings of grains, obtained by letting the grains lose their kinetic energy and come to rest, generically isostatic? The only quantitative study we are aware of is that of Silbert et al. [125], where these authors perform Molecular Dynamics simulation of *monodisperse* grains with a specific form of contact dynamics and a certain energy dissipation coefficient at each collision. The results reported in [125] are compatible with isostaticity for frictionless spheres, $\mu = 0$. In this case, the equilibrium packings are indeed found to obey the condition $n_c = 6$, as expected from the general results of [118,102]. However, when the friction coefficient is non zero, these authors find that the static configurations are such that (a) the fraction of fully mobilized contacts is $\varphi = 0$ and (b) the number of contacts per grain seems to saturate, in the limit of hard grains, to a value of $n_c > 4$, suggesting that the packing is not isostatic. The value of n_c appears to depend significantly on the value of the friction coefficient and the restitution coefficient; it appears from their data that smaller restitution coefficients (i.e. more damping) lowers the value of n_c, perhaps down to the isostatic limit for large damping. This dependence on the details of the dynamics indicates that no universal statement about the statistics of 'native' packings (i.e. obtained without further tapping) can be made. Again, the simplistic situation discussed in section I B 2 would provide a useful benchmark.

What happens when one of these native states (possibly hyperstatic) is vibrated? Does the packing wander inside the stable regime (see Fig. 4) or remains near the isostatic boundary ? Here again, it is useful to recall the results of mean field p-spin

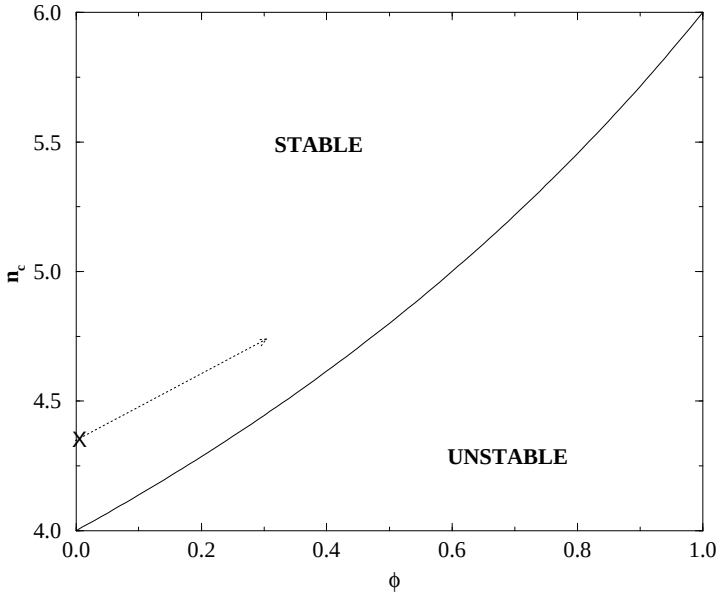

FIG. 4. Stability diagram in the plane φ, n_c for three dimensional assemblies. The plain line is the isostatic line that separates stable packings from unstable packings. The point $\varphi = 1$, $n_c = 6$ corresponds to frictionless particles. The cross for $\varphi = 0$ represents the numerical result of [125]; the dotted arrow is a possible path of the packing when vibrated.

glasses, where the 'vibrations' (temperature) keep the system along the ridge of marginally stable states. In this case, the reason is the exponential dominance of the number of these states over the 'deeper' (more stable) ones. Therefore, even if blocked states are a priori equiprobable (as postulated by Edwards), the most probable situation is to observe the system in a marginal state. If this argument can be transposed to granular packings, then ideas that Edwards expressed in different contexts (i.e; that blocked states are equiprobable and that only marginal (isostatic) states are important [14]) would be reconciled. It would be very interesting to compute the number of metastable states as a function of the isostatic index n_c in some (possibly artificial) model (on this point, see the attempt in [99]).

V. A STRESS-ONLY APPROACH TO GRANULAR MEDIA

We now turn to the discussion of some plausible 'stress-only' closure schemes for the static equilibrium of granular materials. We first start by a natural generalization of the scalar q-model to account for the vectorial nature of the forces. Then we show how the results of this 'vectorial' q-model can be interpreted more generally in terms of symmetry arguments.

A. A vectorial q-model

It is useful to start with a simple toy model for stress propagation, which is the analogue of the scalar model presented in section II. We now consider the case of three downward neighbours (see figure 5), for a reason which will become clear below. Each grain transmits to its downward neighbours not one, but two force components: one along the vertical axis t and one along x, which we call respectively $F_t(i,j)$ and $F_x(i,j)$. For simplicity, we assume that each 'leg' emerging from a given grain can only transport the force parallel to itself. This assumes that each contact is frictionless. More general transfer rules can be considered, where the forces are chosen, *à la* Edwards, randomly within the space of solutions – see e.g. [63,131,105,28].

We assume that a fraction p of the vertical force travels through the middle leg. Correspondingly, a fraction $q_+ = (1-p)(1+\varepsilon)/2$ travels through the right leg, and a fraction $q_- = (1-p)(1-\varepsilon)/2$ through the left leg, so that $p + q_+ + q_- = 1$. (Some anisotropic generalizations will be discussed below). Since the total force in these legs is oriented in the direction ψ, where ψ is the angle between grains, defined in figure 5, the balance of the horizontal force on the grain i,j imposes a specific value for ε:

$$\varepsilon \equiv \frac{1}{(1-p)\tan\psi}\frac{F_x(i,j)}{F_z(i,j)}. \tag{55}$$

We therefore discover a very important consequence of the existence of a shear stress F_x, which was totally absent from the scalar q-model or had to be put by hand: any non zero value of F_x necessarily leads to $q_+ \neq q_-$ and biases the propagation of

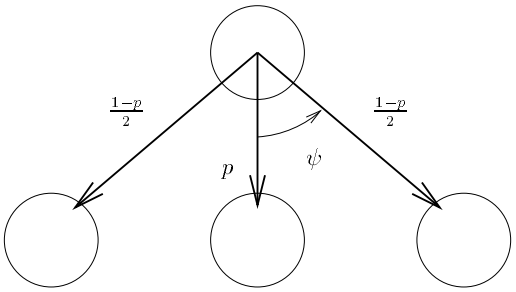

FIG. 5. Three neighbour configuration. Each grain transmits two force components to its downward neighbours. A fraction p of the vertical component is transmitted through the middle leg.

F_z in the direction of F_x. This coupling between the two components of the force is at the origin of all the interesting physics discussed below.

Using the value of ε to compute the propagation of the forces from one layer to the next, we find:

$$\begin{aligned} F_x(i,j) &= \frac{1}{2}\left[F_x(i-1,j-1) + F_x(i+1,j-1)\right] \\ &\quad + \frac{1}{2}(1-p)\tan\psi\left[F_t(i-1,j-1) - F_t(i+1,j-1)\right] \end{aligned} \tag{56}$$

$$\begin{aligned} F_t(i,j) &= w_0 + pF_t(i,j-1) + \frac{1}{2}(1-p)\left[F_t(i-1,j-1) + F_t(i+1,j-1)\right] \\ &\quad + \frac{1}{2\tan\psi}\left[F_x(i-1,j-1) - F_x(i+1,j-1)\right] \end{aligned} \tag{57}$$

Taking the continuum limit of the above equations leads to:

$$\partial_t F_t + \partial_x F_x = \rho + a\frac{1-p}{2}\,\partial^2_{tt} F_t \tag{58}$$

$$\partial_t F_x + \partial_x \left[c_0^2 F_t\right] = \frac{a}{2}\,\partial^2_{xx} F_x \tag{59}$$

where $c_0^2 \equiv (1-p)\tan^2\psi$, a is the size of the grains, and we have kept the second order diffusion terms, which would be the only remaining term in the isotropic scalar description, and plays the role of a smoothing term for the (singular) solutions found below. Comparing Eq.(58) with Eq. (45) (with $w = F_t$), we see that the 'velocity' term introduced by hand in the Edwards model is indeed a consequence of the local shear.

Eliminating (say) F_x between the above two equations leads to a *wave equation* for F_t (up to a diffusion term which becomes small in the large scale limit), where the vertical coordinate t plays the rôle of time and c_0 is the equivalent of the 'speed of light'. In particular, the stress does not propagate vertically, as it does in the scalar model, but rather along two rays, each at a *non zero angle* $\pm\varphi$ such that $c_0 = \tan\varphi$. Note that $\varphi \neq \psi$ in general (unless $p = 0$); the angle at which stress propagates has nothing to do with the underlying lattice structure and can take any value depending on the local rules for force transmission. The three-leg model was chosen to illustrate this particular point: the number of legs is irrelevant in the large scale limit, and the wave structure of the resulting equation is universal.

B. A constitutive relation between stress components

The above derivation can be reformulated in terms of classical continuum mechanics as follows. Considering all stress tensor components σ_{ij}, the equilibrium equation reads,

$$\partial_t \sigma_{tt} + \partial_x \sigma_{xt} = \rho \tag{60}$$

$$\partial_t \sigma_{tx} + \partial_x \sigma_{xx} = 0 \tag{61}$$

Identifying the local average of F_t with σ_{tt} and that of F_x with σ_{tx}, we see that the above equations (58, 59) are actually identical to (60, 61) provided $\sigma_{tx} = \sigma_{xt}$ (which corresponds to the absence of local torque) and, more importantly, that there exists a relation between the vertical and horizontal components of the stress tensor:

$$\sigma_{xx} = c_0^2\,\sigma_{tt} \tag{62}$$

This relation between normal stresses was postulated in [18] as the simplest "constitutive relation" among stress components, obeying the correct symmetries, that one can possibly assume. The term "constitutive relation" normally refers to a relation between stress and strain, but the model under discussion has no strain variables defined. This particular choice can be interpreted as a *local* Janssen approximation [82], in analogy with the assumption made by Janssen in 1895 in order to describe stresses in silos, where the *average* vertical stress at a given altitude is postulated to be proportional to the average horizontal stress. We return later to a more detailed discussion of this type of closure equations. In the present case, the parameter c_0^2 encodes relevant details of the local geometry of the packing (friction, shape of grains, etc.) and may thereby depend on the *construction history* of the grain assembly. Only for simple, 'homogeneous' histories (such as constructing a uniform sand-bed using a sieve) will c_0^2 be everywhere constant on the mesoscopic scale. Even then, unless an ordered packing is somehow created, local fluctuations of c_0^2 will always be present. The influence of these fluctuations will be analyzed below.

C. Some simple situations

Using Eq.(62) in Eqs. (60, 61) we find that these can be rewritten as:

$$\partial_u(\sigma_{xt} - c_0\sigma_{tt}) = -\frac{\rho}{2} \tag{63}$$

$$\partial_v(\sigma_{xt} + c_0\sigma_{xt}) = \frac{\rho}{2}, \tag{64}$$

where $u = x - c_0 t$ and $v = x + c_0 t$. This shows that in this framework, the forces are transported along the characteristics, which is what the word 'force chain' usually implies [61,35]. More precisely, the solution of Eqs. (60, 61) is obtained by projecting any 'initial' force (i.e. present at altitude $t = 0$) onto the two characteristics, and propagating and augmenting each component by an amount $(\rho/2)\mathrm{d}t$, independently along these characteristics.

The simplest situation is that of an infinitely wide layer of sand, of depth H, with a localized (δ-function) overload at the top. The additional weight at the bottom then defines the *response function* of the wave equation, which, in two dimensions, is the sum of two δ peaks localized at $x = \pm c_0 H$. These δ peaks are actually diffusively broadened by the second order terms present in Eqs. (58, 59). This two-peak response function is notably different from the response function of an isotropic elastic body, for which the response function is a single hump of width proportional to the height H. However, for anisotropic elasticity, a two peak response function *can* be observed [73,68,110], but both peaks have a width scaling linearly with H, and not as $H^{1/2}$ for an hyperbolic equation. The question of the response function is therefore of crucial importance, and will be discussed in details below. Recent attempts to determine the response function experimentally seem to favor an elastic like response, at least for the strongly disordered systems (see section VI).

Next, one can consider the sandpile geometry. For a pile at repose, the position of the free surfaces are $x = \pm cz$, where $c = \cot\phi$ with ϕ the repose angle. On these surfaces, all the stresses vanish. This boundary condition is then (for given c_0 and c) sufficient to solve for the stress field everywhere in the pile. One then finds that the vertical normal component of the stress is piecewise linear as a function of x. In particular, for $-c_0 H \le x \le c_0 H$, σ_{tt} is *constant*. Therefore, in two dimensions, this model [18] predicts a flat-topped stress profile rather than a hydrodynamic pressure hump or a dip. Such a flat top is in fact observed when building a pile from a uniform rain of grains.

For a pile created by depositing grains from above (for example by sieving sand onto a disc) it is natural to expect the free surface to be a slip plane. (This is a plane across which the stress components saturate the Mohr-Coulomb condition – see below.) Interestingly, this provides a relation between c_0 and the friction angle ϕ, which reads: $c_0^2 = 1/(1 + 2\tan^2\phi)$ (note that since $c = 1/\tan\phi$, one has automatically $c > c_0$). Under these conditions one finds that the 'plastic' region (where the Mohr-Coulomb condition is saturated) extends (in two dimensions) inward from the surface to encompass the outer 'wings' of the pile (i.e. $c_0 z \le |x| \le cz$). This follows from the solution of the model and is not an *a priori* assumption, of the kind commonly made in elastoplastic modeling (e.g., [33,123]; see also the discussion in [104]). In three dimensions, a second closure relation is required [18], but in all cases the stress profile has a broad maximum at the center of the pile. Now, however, the Mohr-Coulomb condition is only saturated in the immediate vicinity of the free surface – the 'plastic' region has zero volume in three dimensions [18,146].

D. Symmetries and Constitutive Relations

Although above it was motivated in the context of a specific microscopic model of force transfer, the linear constitutive relation (62) can be viewed, independently of any microscopic model, as the simplest closure equation compatible with the symmetries of the problem. The latter include a *local* reflection symmetry in which $x - x_0$ is changed to $x_0 - x$ (with x_0 an arbitrary reflection plane) and also a form of "dilational" symmetry on the stress known as RSF ("radial stress field") scaling. RSF scaling depends on the absence of any characteristic stress scale, which follows if the Young's modulus of the grains is sufficiently much larger than any stresses arising in the granular assembly being studied. Such scaling, which requires the stress

distributions beneath piles of different heights to have the same shape, is quite well confirmed in some (but not all) experiments on conical sand-piles [128,29,123].

Even with these two symmetries, one can consider more complicated (nonlinear) constitutive relations among stresses, which must be of the form [18]:

$$\sigma_{xx} = c_0^2 \sigma_{tt} \, \mathcal{F}\left(\frac{\sigma_{xt}^2}{\sigma_{tt}^2}\right). \tag{65}$$

Note that in general, such a constitutive relation violates rotational symmetry, and can only describe an anisotropic pile (for example, built from a rain of grains under gravity). The only rotationally invariant stress only closure scheme can only involve the two invariants of the stress tensor, namely $\mathrm{Tr}\,\sigma$ and $\mathrm{Det}\,\sigma$. From dimensional analysis, this relation can only be of the form:

$$\cos^2\phi (\mathrm{Tr}\,\sigma)^2 = 4\mathrm{Det}\,\sigma, \tag{66}$$

where the specific choice of the coefficient is such that we recognize the usual Mohr-Coulomb relation. Eq. (66) indeed means that there exists a choice of orthogonal axis m, n such that:

$$\left|\frac{\sigma_{nm}}{\sigma_{nn}}\right| = \tan\phi = \mu, \tag{67}$$

where μ is the internal friction coefficient. One can easily show that this relation is of the general form Eq. (65), for a particular form of $\mathcal{F}$, since Eq. (66) can also be rewritten such as:

$$c_0^2 \, \mathcal{F}(u) = \frac{1}{\cos^2\phi}\left[\sin^2\phi + 1 \pm 2\sin\phi \, \sqrt{1 - \cot^2\phi \;\; u}\right] \tag{68}$$

Viewed as a constitutive equation, the Mohr-Coulomb relation defines a rigid-plastic model whose physical content is to assume that, everywhere in the material, a plane can be found across which slip failure is about to occur, hence the name "incipient failure everywhere", (IFE), given to this model [18,145,146].

All closures of the form (65) lead to hyperbolic equations for stresses, although in the general case the characteristic directions of propagation (the 'light rays' of the corresponding wave equation) depend on the loading and therefore vary with position.

An interesting situation arises when local reflection symmetry is broken. This is the case, for example, in sand-piles created by pouring from a point source onto a rough surface – which is the usual mode of construction. In such a pile, all grains arriving at the apex of the pile roll (in two dimensions) either to the right or to the left. The two halves of the pile therefore have different construction histories that are mirror images of each other. This violates local reflection symmetry, and in general permits constitutive equations such as:

$$\sigma_{xx} = c_0^2 \sigma_{tt} \, \mathcal{G}\left(\frac{\mathrm{sign}(x)\sigma_{xt}}{\sigma_{tt}}\right) \tag{69}$$

The simplest case (found e.g. by expanding $\mathcal{G}$ to first order in the shear to normal stress ratio) corresponds to a family of (quasi-) linear constitutive relations [146]:

$$\sigma_{xx} = c_0^2 \sigma_{tt} + \nu \, \mathrm{sign}(x)\sigma_{xt} \tag{70}$$

The previous, symmetrical, case has $\nu = 0$. For nonzero ν, (70) again leads to a wave equation, although this time *anisotropic*, in the sense that the two characteristic rays make asymmetric angles to the vertical axis. Note also that $x = 0$ is a singular line across which the directions of propagation change discontinuously.

Microscopically, $\nu \neq 0$ leads to an unequal sharing of the weight of a grain between the two characteristic rays propagating downward from it. Such a model can indeed be obtained from rules such as those in figure 5 simply by having an asymmetric rules for partitioning the forces between the supporting grains, for example choosing two different angles ψ_+ and ψ_-. The symmetric case corresponds to $\nu = 0$ and $\nu \propto \tan\psi_+ - \tan\psi_-$. For $\nu < 0$, most of the weight travel *outwards* on the leg with the smallest opening angle; this provides, within a fully tensorial model, a mathematical description of the tendency to form arches, as developed by Edwards for the scalar case.

Solving these anisotropic wave equations for sand-piles in two dimensions one again finds for σ_{tt} a piecewise linear function, which now has a maximum at $x = 0$ when $\nu > 0$, but a minimum for $\nu < 0$, in accord with the arching picture mentioned above. If one furthermore imposes, as above, that the free surfaces are slip planes, one finds a relation between c_0^2, ν and ϕ. One again finds the result that the material throughout the outer wings of the pile (exterior to the triangle formed by the characteristics passing through the apex) are at incipient (Mohr-Coulomb) failure.

E. Boundary conditions and 'fragility'

All the above closure schemes lead to hyperbolic equations, which crucially differ from the elliptic equations encountered in elasticity theory when *boundary conditions* are considered. Hyperbolic equations indeed require only 'half' of the boundary conditions to be specified, the other half being *determined* by 'propagating' these known boundary conditions along the characterisitcs through the system. On the contrary, an elliptic equation (such as Laplace's equation) requires the stress (or the displacement) on all the surfaces of the body to be specified. If one insists on applying all the boundary conditions appropriate to an elastic body, then in general no solution will exist for the hyperbolic equations that correspond to a particular choice of constitutive relation. If these boundary conditions are 'incompatible' in this sense, then within an hyperbolic model, the material ceases to be in static equilibrium. This is not different from the corresponding statement for a fluid; if boundary conditions are applied that violate the conditions for static equilibrium, some motion will result. Unlike a fluid, however, for a granular medium we expect such motion to be in the form of a finite rearrangement rather than a steady flow. Such a rearrangement will change the micro-texture of the material, and thereby *alter the constitutive relation among stresses*. One expects it to do so in such a way that the new (spatially inhomogeneous) constitutive relation becomes compatible with the imposed forces.

Within this modeling approach, a granular assembly is therefore able to support some, but not all, of the surface loads that would be supportable by an elastic medium. Such models may therefore provide an interesting paradigm for the behaviour of "fragile matter" [35].

VI. EXPERIMENTAL AND NUMERICAL DETERMINATION OF THE STRESS RESPONSE FUNCTION

The stress 'response function' to a localized overload is of prime interest both from a fundamental point of view but also for many engineering applications. On large scales, the extra stresses created by a house within the soil beneath it are indeed related to this response function. Therefore, this problem has received considerable theoretical attention in the engineering community, where, as mentioned in the introduction, the granular material is often assumed to be a (possibly anisotropic) elastic material. Note that an elliptic response function corresponds to a favorable case for stability since the stresses are efficiently dispersed in space, whereas a hyperbolic response function would lead to a rather localized stress field.

In spite of its importance, the response function of granular assemblies has only very recently been measured experimentally [69,116,103]. Various methods were used: one is a direct quantitative measurement of the response at the bottom of a 3D packing using a local stress probe based on the deformation of a hard membrane [116], another method is based on carbon paper imprints created by a monodisperse 3D packing [103]. For 2D packing the photo-elastic response of polymeric grains was used [69] in order to evidence the inter-particle force path. This is a semi-quantitative method but it allows to visualize directly the response in the bulk as well as the topology of the path followed by the stress chains. Such an observation will be used to built the theoretical proposition exposed in the following section. These experimental efforts have lead so far to the following picture[2]: for strongly disordered packings (for example by considering mixtures of grains of very different sizes, or irregular grains such as natural sand), the response profile on large length scales shows a single broad peak [69,116]. This single hump response function was also observed in numerical simulation of 2D polygonal grains packing [101].

For well ordered packings however, the two peaks structure is rather convincingly observed in two dimensions (a 'ring' or three peaks in $3D$) [69,103,15]. These hyperbolic features are also in agreement with a recent numerical simulation on (rather small) isostatic assemblies of frictionless grains [138,78], with the work reported in [63,28] where beads are arranged on a regular triangular lattice but where disorder is introduced by a finite friction coefficient. Similarly, two-peak response can be observed for strongly anisotropic elastic networks [73,110].

Obtaining a precise experimental determination of the linear response function that can be *quantitatively* compared to theoretical models is rather difficult: the perturbation must be small enough not to disrupt the packing, but also large enough to lead to a measurable signal. A very sensitive technique, based on a lock-in detection of an oscillating perturbation, has allowed one to obtain precise and reproducible results [116,124]. One finds unambiguously that the response function $G(r, H)$ to a perturbation located at $r_0 = z_0 = 0$ is in the case of sand layers *single-peaked*, with a width growing as the height H of the layer. More precisely, the response function for different heights can be rescaled onto a unique curve by plotting $H^2 G(r, H)$ as a function of r/H. The factor H^2 is expected from force conservation: the integral of the response function over the bottom plate must be equal to the overload force F for the total force to balance. One also finds that, like for sand-piles, the pressure response profile depends on the way the granular layer was prepared – its 'history': the value of the maximum of this response is roughly twice smaller (and its width twice larger) for a dense packing than for a loose one (see Fig. 6). The quantitative shape

[2]Note however that a purely 'diffusive' response function, scaling as $\sqrt{H}$ as predicted by the 'scalar' model, was reported in [126] for a very special 'brick' packing.

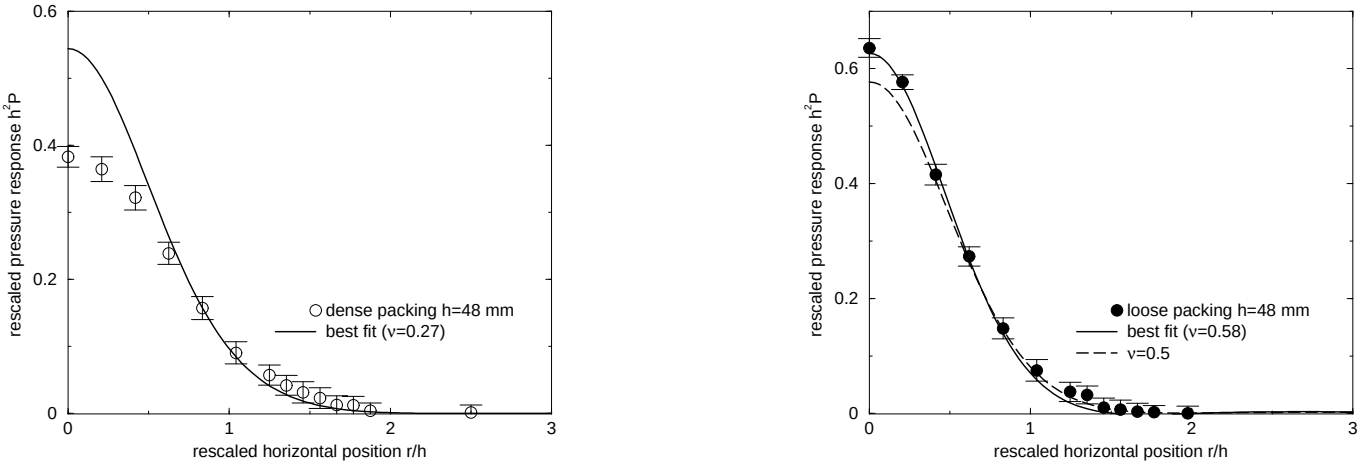

FIG. 6. Left: Fit of the 'dense' packing data with the standard elastic Green function. The agreement is not good at all. Right: Fit of the loose packing data. The best fit value for ν exceeds the elastic bound $\nu \leq \frac{1}{2}$. From [124].

of the experimental response function cannot be accounted for by a simple isotropic elasticity theory (see also the discussion in [147]), but in the present geometry, anisotropic elasticity leaves three extra adimensional constants that can give a large freedom to fit the data (see [110]).

Therefore, the most precise experiments on strongly disordered packings seems to favor a single peak, elastic like response, rather than a double peak response that only appears in special conditions (ordered packings, or frictionless grains). We therefore need to understand in details the rôle of randomness in hyperbolic wave equations, or in more physical terms, the large scale consequence of the fact that force chains are 'scattered' by packing irregularities. Is this sufficient to convert a two peak response function into a single peak, elastic like function? This is the subject of the following sections.

VII. FORCE CHAINS SCATTERING I: WEAK DISORDER LIMIT

A. A stochastic wave equation

Provided that local conservation laws (those arising from mechanical equilibrium) are obeyed, many local rules for force transmission are *a priori* compatible with the existence of contacts among rigid particles [63,131]. Therefore, even if there is a definite mean relationship among stresses at the meso-scale, one can expect randomness in the local transmission coefficients. The simplest model for this and other sources of randomness is to introduce a randomly varying 'speed of light' c_0. This could describe the fact that, for example, the parameter p in the model of figure 5 can vary from grain to grain. In this situation the two rays are still symmetric around the vertical direction, but with a random opening angle. The situation where the bisecting line itself is random (i.e. when both the above opening angles $\psi_\pm$ are fluctuating) will be alluded to below.

This suggests the following stochastic wave equation for stress propagation in two dimensions:

$$\partial_{tt}\sigma_{tt} = \partial_{xx}\left[c_0^2(1+v(x,t))\ \sigma_{tt}\right] \tag{71}$$

where the random noise v is assumed to be correlated as $\langle v(x,t)v(x',t')\rangle = \sigma^2 g_x(x-x')g_t(t-t')$. The correlation lengths ℓ_x and ℓ_t are again kept finite, and of the same order of magnitude. In Fourier transform, this relation can also be written $\langle v(k,t)v(k',t')\rangle = 2\pi\sigma^2\delta(k+k')\tilde{g}_x(k)g_t(t-t')$. It turns out that the final shape of the averaged response function depends on the sign of $\tilde{g}_x(\Lambda)$. In section III we implicitly made the choice $\tilde{g}_x(k)=1$, which corresponds to: $g_x(x=0)=1/a$ and $g_x(x>0)=0$. We will keep this choice for the following calculations, but note that another form for g_x could lead to $\tilde{g}_x(\Lambda))<0$.

In the following, σ_{tt} will be again denoted by w. After a Fourier transform along x-axis, we get, from equation (71)

$$(\partial_{tt}+c_0^2k^2)w = \partial_t\rho - c_0^2k^2\int\frac{dq}{2\pi}w(q,t)v(k-q,t) \tag{72}$$

Note that the 'source' term of this equation is now $\partial_t\rho$ rather than ρ itself. Therefore, if we call G the Green function (or propagator) of this equation $G=\langle\delta w/\delta\partial_t\rho\rangle$; the response function $R=\langle\delta w/\delta\rho\rangle$ of our system is now actually the time derivative of G: $R(k,t)=\partial_t G(k,t)$.

The noiseless propagator G_0 is the solution of the ordinary wave equation $(\partial_{tt} + c_0^2 k^2) G_0(k, t-t') = \delta(t-t')$ and can be easily calculated:

$$G_0(k,t) = \frac{1}{2\imath c_0 k} \left[e^{\imath c_0 k t} - e^{-\imath c_0 k t} \right] \theta(t) \tag{73}$$

which leads to the response function R_0

$$R_0(x,t) = \frac{1}{2} \left[\delta\left(x - c_0 t\right) + \delta\left(x + c_0 t\right) \right] \theta(t) \tag{74}$$

This last equation sums up one of the major results of the hyperbolic approach of [18,145,146]: in two dimensions, stress propagates along two characteristic rays. (Note that the corresponding response function in three dimensions reads $R_0(x,t) \propto (c_0^2 t^2 - x^2)^{-1/2}$ for $|x| < c_0 t$ and zero otherwise [18]). A relevant question is now to ask how these rays survive in the presence of disorder. We will show that for weak disorder, the δ-peaks acquire a finite (diffusive) width, and that the 'speed of light' is renormalized to a lower value. Not surprisingly, the effect of disorder can be described by an 'optical index' $n > 1$. For a strong disorder, however, we find (within a Gaussian approximation for the noise v) that the speed of light vanishes and becomes imaginary. The 'propagative' nature of the stress transmission disappears and the system might behave more like an elastic body, in a sense clarified below.

B. Calculation of the averaged response function

One can again use Novikov's theorem in the present case if the noise is Gaussian and short range correlated in time. However, the same results are again obtained within the diagrammatic approach explained in section III, which can be easily transposed to the present case, and is more general. The propagator G is a now represented as a line, the source $\partial_t \rho$ a cross and the vertex meaning $-c_0^2 k^2 \int \frac{dq}{2\pi}$. Within the MCA, the self-consistent equation (analogous to equation (38) in the scalar case) is:

$$(\partial_{tt} + c_0^2 k^2) H(k,t) = \delta(t) + \int_0^t dt' \Sigma_{\text{MCA}}(k,t') H(k, t-t') \tag{75}$$

where H is defined by $G(k,t) = H(k,t)\theta(t)$, and the self-energy Σ_{MCA} given as

$$\Sigma_{\text{MCA}}(k, t-t') = 2\pi c_0^4 \sigma^2 k^2 \int \frac{dq}{2\pi} q^2 g_t(t-t') \tilde{g}_x(k-q) H(q, t-t') \tag{76}$$

Equation (75) can be solved using a standard Laplace transform along the t-axis (E is the Laplace variable). Using the fact that $H(k,\tau) = \tau$ in the limit where $\tau \to 0$, we find, for small k, E (corresponding to scales L such that $\ell_x,\ \ell_t \ll L$): $H^{-1}(k,E) = E^2 + \beta E + c_R^2 k^2$, where

$$c_R^2(k) = c_0^2 - \frac{c_0^4 \sigma^2 \Lambda^3 \ell_t}{6} \left(1 - \frac{3|k|}{2\Lambda} \right) + \mathcal{O}(k^2) \tag{77}$$

$$\beta(k) = \frac{c_0^4 \sigma^2 k^2 \Lambda^3 \ell_t^2}{9} + \mathcal{O}(k^3) \tag{78}$$

We notice here that in the limit $\ell_t \to 0$, the effect of the randomness completely disappears, as in the scalar model with the Ito convention. (Technically, this is due to the fact that $G(k, t=0) \equiv 0$ in the present problem). In order to calculate the inverse Laplace transform, we need to know the roots of the equation $H^{-1}(k,E) = 0$. This leads to several phases, depending on the strength of the disorder.

- The weak disorder limit.

For a weak disorder, $c_R^2(k)$ is always positive. We can then define $c_R = c_R(k=0)$. As we will show now, c_R is the shifted 'cone' angle along which stress propagates asymptotically. c_R is a decreasing function of σ, meaning that the peaks of the response function get closer together as the disorder increases [3]. For a critical value $\sigma = \sigma_c$, c_R vanishes, and becomes imaginary for stronger disorder.

---

[3] As a technical remark, let us note that if $g_t = g_x$, the problem is symmetric in the change $x \to t$, $c^2(x,t) \to 1/c^2(x,t)$. It thus looks as if the cone should both narrow or widen, depending on the arbitrary choice of x and t. There is however no contradiction with the above calculation since we assumed that v has zero mean, while $1/(1+v) - 1$ has a positive mean value, of order σ^2

In the limit of large t, the propagator reads:

$$G(k,t) = \frac{1}{c_R k} \sin\left[c_R k t(1+\alpha|k|)\right] e^{-\gamma k^2 t}\theta(t) \tag{79}$$

where the following constants have been introduced [4]:

$$\alpha = \frac{3}{4\Lambda}\left(\frac{c_0^2}{c_R^2} - 1\right) \tag{80}$$

$$\gamma = \frac{\beta(k)}{2k^2} = \frac{\sigma^2 \Lambda^3 \ell_t^2}{18} \tag{81}$$

From equation (79), the response function R, in the limit of small k and large t, is given by:

$$R(k,t) = \cos\left[c_R k t(1+\alpha|k|)\right] e^{-\gamma k^2 t}\theta(t) \tag{82}$$

or in the real space,

$$R(x,t) = \frac{1}{2\sqrt{4\pi|\hat{\gamma}|(t)}} \Re\left\{ \frac{e^{-\xi_+^2/b}}{\sqrt{b}}\left[1 - \Phi(-\imath\frac{\xi_+}{\sqrt{b}})\right] + \sqrt{b}\, e^{-b\xi_-^2}\left[1 - \Phi(-\imath\sqrt{b}\xi_-)\right]\right\} \tag{83}$$

where the scaling variables $\xi_\pm$, measuring distances relative to the two peaks, are defined by

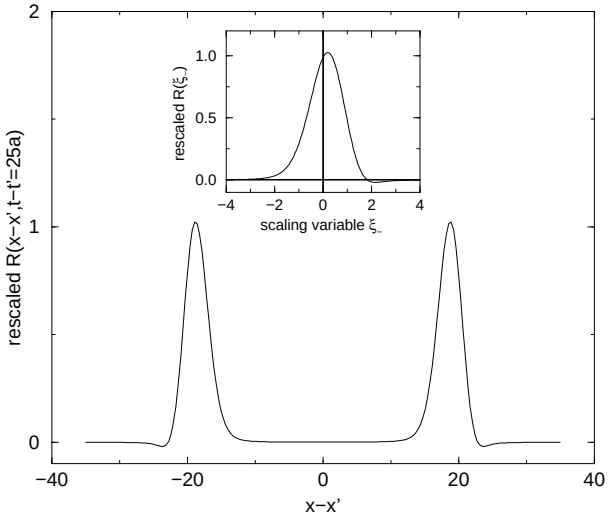

FIG. 7. Response function for weak disorder ($\sigma/\sigma_c \sim 0.32$). The two curves have been rescaled by the factor $2\left[4\pi|\hat{\gamma}|t\right]^{1/2}$. The main graph shows the general double-peaked shape of the response of the system when subjected to a peaked overload at $x = 0,\ t = 0$. The inset gives details the right-hand peak as a function of the scaling variable ξ_-. Note the asymmetry (for $\tilde{g}_x(\Lambda) > 0$), compatible with the results found in [63]. Note also that the curve becomes negative around $\xi_- = 2$.

$$\xi_\pm = \frac{x \pm c_R t}{\sqrt{4|\hat{\gamma}|t}} \tag{84}$$

and where $\hat{\gamma} = \gamma - \imath c_R \alpha$, $b = e^{\imath \arg\hat{\gamma}}$. Φ is the standard error function. Figure 7 shows R as given by expression (83). Interestingly, this propagator not only has a finite diffusive width $\propto \sqrt{t}$, but is also asymmetric around its maxima. Surprisingly, and in sharp contrast to the scalar case discussed above, the response function becomes *negative* in certain intervals (although its integral

[4]Note that the sign of α is dictated by the sign of $\tilde{g}_x(\Lambda)$

is of course equal to one because of weight conservation). This means that pushing on a given point actually reduces the downward pressure on certain points. This can be interpreted as some kind of arching: increasing the shear stress does affect the propagation of the vertical stress, and may indeed lead to a reduction in its local value which is redistributed elsewhere. The un-averaged response function therefore necessarily takes negative (and in fact rather large [41]) values. This is actually of crucial importance since this is the source of fundamental 'fragility' of granular matter to external perturbations. Suppose indeed that as a result of the perturbation, a grain receives a negative force larger than the preexisting vertical pressure. This grain will then move and a local rearrangement of contacts will occur, inducing a variation of $c_0(x,t)$ as to reduce the cause of the instability. Thus, the stochastic wave equation implicitly demands rules similar to those introduced, e.g. in [40]. The present model, which is purely static, does not say what to do when a local rearrangement occurs, but certainly suggests that small perturbations should induce such rearrangements.

It is interesting to note that this response function was numerically measured in [63]; its shape is compatible with the above expression; in particular, the two peaks were found to be asymmetric with a longer 'tail' extending inwards, as we obtain here. Note however that for $\tilde{g}_x(\Lambda) < 0$, the shape of the peaks is reversed: the small dips are located inside the peaks and the longer tail extends outwards. In a more recent work [28], both the diffusive spreading and the renormalisation of the wave velocity have been observed.

• Critical disorder: The wave/diffusion transition.

When the disorder is so strong that c_R just vanishes, the roots of $H^{-1}(k,E) = 0$ change nature, and so does the response function R. The two peaks of the previous expression for R merge together, while the width becomes anomalously large ($\propto t^{2/3}$). In the asymptotic, large t, regime we obtain:

$$R(k,t) = \theta(t) \cos\left[\lambda |k|^{3/2} t\right] e^{-\gamma k^2 t} \tag{85}$$

where the new constant λ is defined by $\lambda = c_0\sqrt{3/2\Lambda}$ and $\gamma = c_0^2 \ell_t/3$.

• Strong disorder: The pseudo-elastic regime.

For larger disorder still, one finds, within the MCA (which is exact for a Gaussian, uncorrelated noise), that the renormalized value of c_0^2, c_R^2, becomes negative. Upon a rescaling of x as $\hat{x} = x/(ic_R)$, the effective equation on $\langle \delta\sigma_{tt} \rangle$ then becomes, on large length scales, Poisson's equation:

$$\nabla^2 \langle \delta\sigma_{tt} \rangle = \partial_t \langle \delta\rho \rangle \tag{86}$$

which means that the stress propagation becomes somewhat similar to that in an elastic body, where stresses obey an elliptic equation of similar type [89]. In particular, the cone structure of stress propagation, which is associated with the underlying, hyperbolic, wave equation finally disappears; the average response to a localized perturbation becomes a broad 'bump' of width comparable to the height of the pile. However, the above transition is possibly an artifact, due to the fact that v is taken to be Gaussian, which strictly speaking is not allowed, since the local value of c_0^2 should always be positive. One can show for some other problems of the same type that a similar transition is artificially induced by the Gaussian approximation when it cannot really exist on physical grounds. We need to address the strong disorder limit with different tools in order to discuss the large scale nature of the response function in this case: this will be discussed below.

C. Generalized wave equations

It is tempting to generalize equations (58, 59) and write the most general linear equations governing the propagation of the forces which are compatible with the (local) conservation rules. These equations were first written by de Gennes [70]:

$$\partial_t F_t + \partial_x \left[\eta'(x,t) F_x + \nu'(x,t) F_t\right] = \rho \tag{87}$$

$$\partial_t F_x + \partial_x \left[\eta(x,t) F_t + \nu(x,t) F_x\right] = 0 \tag{88}$$

Note that the terms ν, ν' break the symmetry $x \to -x$, and exist whenever the transfer rules in the three leg model are not symmetrical. Equations (87, 88) describe a situation where not only the opening angle of the cone can vary in space, but also its average orientation.

The same analytical techniques as above can still be used. We shall only discuss some special cases [5]:

[5] To lowest order in perturbation theory, the case where disorder is present in the four terms η, η', ν, ν' simultaneously is very simply obtained by adding the corrections induced by each term taken individually.

∘ Let us first set $\nu = \nu' = 0$ and consider the case where η' is random, and η fixed (and equal to c_0^2). Taking $\eta'(x,t) = \eta'_0\ (1 + v(x,t))$ with the noise v as above, one finds that the renormalized value of η' is:

$$\eta'_R = \eta'_0 \left(1 - \frac{c_0^2 \eta'_0 \sigma^2 \Lambda^3 \ell_t}{6}\right) \tag{89}$$

Now, on large length scales, one must recover the continuum equilibrium equations for the stress tensor, equations (60, 61). The condition of zero torque requires that the stress tensor is symmetric, and thus one must set $\eta'_R \equiv 1$, which imposes a relation between η'_0 and the amplitude of the noise σ. Note that beyond a certain value of σ, this relation can no longer be satisfied with a real η'_0. This again means that the packing is unstable mechanically and will rearrange so as to reduce the disorder.

∘ Another interesting class of models, which one can call 'μ models', is such that: $\eta = c_0^2, \eta' = 1$, but $\mu(x,t) = c_0 v(x,t)$ and $\mu' = 0$ or vice-versa. These two cases yield identical results, namely, in the large t limit:

$$R(k,t) = \cos(c_0 k t)\, e^{-\gamma k^2 t} \theta(t) \tag{90}$$

$$R_s(k,t) = -\imath c_0 \sin(c_0 k t)\, e^{-\gamma k^2 t} \theta(t) \tag{91}$$

where $\gamma = \frac{c_0^2 \Lambda \sigma^2}{4}$. Note that in these cases, the response peaks acquire a finite diffusive width $\propto \sqrt{t}$, but the angle of the information cone is unaffected by the disorder (i.e. c_0 is not renormalized).

∘ Finally, there are special 'symmetry' conditions where the equations can be decoupled and reduced to two 'scalar' models. We will refer to this case as the 'double scalar' model. This occurs when $\mu = \mu' = c_0 v_1(x,t)$ and $\eta' = \eta/c_0^2 = 1 + v_2(x,t)$ where v_1, v_2 are two different sets of noise. Let us define $\sigma_\pm = c_0 F_t \pm F_x$, $x_\pm = x \mp c_0 t$ and $v_\pm = v_1 \pm v_2$, we then obtain:

$$\partial_t \sigma_+ = c_0 \rho - c_0\ \partial_{x_+}[v_+ \sigma_+] \tag{92}$$

$$\partial_t \sigma_- = c_0 \rho - c_0\ \partial_{x_-}[v_- \sigma_-] \tag{93}$$

showing that σ_+ and σ_- decouple, each propagating along two rays, of 'velocity' $\pm c_0$, plus a small noise $v_\pm$ which, as in the scalar case, generates a nonzero diffusion constant. The response functions for σ_{tt} and σ_{xt} are thus again made of two diffusive peaks of width $\propto \sqrt{t}$, centered in $x = \pm c_0 t$. Note that by construction, this special form of disorder does not lead to negative vertical stresses.

A physically relevant question is to know how local stresses are distributed. We have seen above that within a scalar approach, an exponential-like distribution (possibly of the type $\exp -w^\beta$, with $\beta \geq 1$) is expected [93,46]. One can wonder whether this exponential distribution survives within a tensorial description, and what happens for very small stresses $w \to 0$. Unfortunately, the full distribution can only be computed analytically for the 'double scalar' model; but numerical results have also been obtained for the random BCC model [41] and confirm that the exponential tail holds in the strong disorder limit.

In the 'double scalar' limit, the histogram of the stress distribution is obtained trivially by noting that since $\sigma_+ = w_1$ and $\sigma_- = w_2$ travel along different paths, they are independent random variables. Taking c_0 to be unity for simplicity, one thus finds:

$$P(\sigma_{tt}) = \int dw_1 \int dw_2 P^*(w_1) P^*(w_2) \delta(\sigma_{tt} - \frac{w_1 + w_2}{2}) \tag{94}$$

$$P(\sigma_{xt}) = \int dw_1 \int dw_2 P^*(w_1) P^*(w_2) \delta(\sigma_{xt} - \frac{w_1 - w_2}{2}) \tag{95}$$

where P^* is the distribution of weight pertaining to the scalar case, which, as mentioned above, depends on the specific form of the local disorder and on the discretisation procedure. In the strong disorder case which leads to equation (8) [in the case $N = 2$], we thus find that $P(\sigma_{tt})$ is still decaying exponentially (it is actually a Γ distribution of parameter $2N$), although its variance is reduced by a factor 2. For $N = 2$, one simply gets

$$P(\sigma_{tt}) = \frac{8}{3} \sigma_{tt}^3 e^{-2\sigma_{tt}} \tag{96}$$

$$P(\sigma_{xt}) = \left(|\sigma_{xt}| + \frac{1}{2}\right) e^{-2|\sigma_{xt}|} \tag{97}$$

The interest of the 'double scalar' limit of the hyperbolic model is to show that the exponential tail Eq. (8) has indeed a certain degree of universality, and is not restricted to the scalar model.

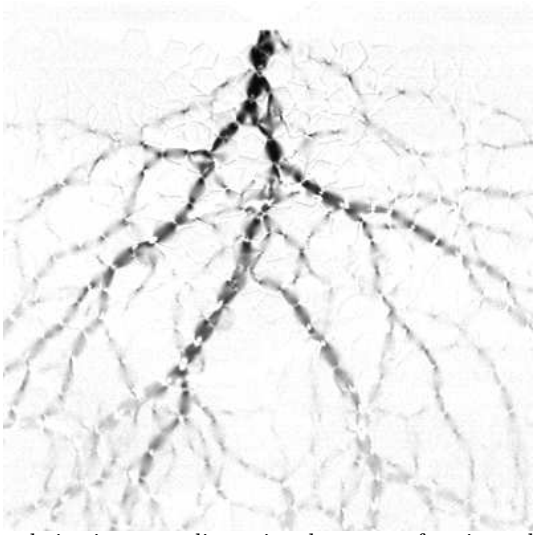

FIG. 8. Picture of the response force chains in a two-dimensional system of grains subject to a vertical force imposed at the middle of the top surface. To get this picture birefringent grains between inverse circular polarizers have been used, and the intensity difference after and before the overloading has been computed. This picture was obtained by R.P. Behringer and J. Geng.

VIII. FORCE CHAINS SCATTERING II: STRONG DISORDER LIMIT

A. Introduction and numerical results

From pictures of photo-elastic grains, the network of inter-particle forces propagating as a responses to a localized pressure was extracted [43,69] (see Figure 8). An interpretation of such a picture can be given in terms of linear force chains which tend to split upon meeting vacancies or packing defects [24].

As reviewed in the previous section, one can investigate perturbatively the role of disorder on hyperbolic equations. In this case, the two peak structure of the response function is preserved on large length scales, although the peaks are diffusively broadened. This result is in qualitative agreement with the numerical simulations [63,78,28]. An uncontrolled extrapolation to strong disorder however suggests that the large scale equations might become elliptic.

In order to investigate more quantitatively the strongly disordered regime where force chains split and merge, one can study [24] the following model. If one of the force chains meets a defect (randomly distributed in space), we split it into two new ones at random angle, which then propagate until another defect (or the boundary) is reached. More precisely, a chain carrying a force f in the direction $\vec{n}$ splits when meeting a defect into two forces f_1, f_2 in the directions $\vec{n}_1$, $\vec{n}_2$ – '⅄ process'. The two angles θ_1 and θ_2 (between $\vec{n}$ and $\vec{n}_1$ and $\vec{n}_2$ respectively) are uniformly chosen between 0 and some maximum splitting angle θ_M. The local mechanical equilibrium imposes that the intensities f_1 and f_2 are such that $f\vec{n} = f_1\vec{n}_1 + f_2\vec{n}_2$. Sometimes, two (or more) force chains meet at the same defect – 'Y process'. In this case, we make them merge together. It is important to note that the positions of the defects are fixed before starting the computation of the forces. This idea of a frozen disorder is consistent with the experimental observation that when the local overload is added on the top of the system, the forces are transmitted along the chains originally created during the building of the packing. In other words, as long as the applied force is not too large and compatible with the pre-existing network of force chains, the geometry of the packing, and in particular the contacts between grains, remains the same (but see the discussion in section IX).

With these rules, realistic force networks can be created numerically [24]. After averaging over many statistically identical samples, one can obtain stress profiles for different heights H. One finds that, as H increases, the vertical pressure response profile evolves continuously from two well defined peaks to a single broad one. It means that the hyperbolic behaviour is progressively erased by multiple scattering. The width of the single peak is found to scale like H; the scaling function is furthermore surprisingly close to the pure elastic response of a semi-infinite two-dimensional medium. However, the numerical simulation was restricted to rather shallow (small H) samples.

B. A Boltzmann description of force chain splitting

In order to understand analytically the above numerical results, we write a Boltzmann equation for the probability density $P(f,\vec{n},\vec{r})$ of finding an oriented force chain of intensity f in the direction $\vec{n}$ around the point $\vec{r}$ [24]. A very important point here is that force chains can be oriented in reference to the boundary conditions (see the discussion in [34,138,24]).

For simplicity, we first neglect the chain 'merging' process which leads to a more complicated non linear Boltzmann equation (its influence is not fully understood yet and will be discussed below). We also assume that the splitting is symmetric, i.e that $\vec{n}\cdot\vec{n}_1 = \vec{n}\cdot\vec{n}_2 \equiv \cos\theta$, so that $f_1 = f_2 = f/2\cos\theta$. Assuming a uniform density of defects, the probability distribution $P(f,\vec{n},\vec{r})$ obeys the following general equation:

$$P(f,\vec{n},\vec{r}+\vec{n}\,dr) = (1-\frac{dr}{\lambda})P(f,\vec{n},\vec{r}) + 2\frac{dr}{\lambda}\int d\vec{n}'\int df' P(f',\vec{n}',\vec{r})\Psi(\vec{n}',\vec{n})\,\delta\left(f-\frac{f'}{2\cos\theta}\right), \tag{98}$$

where λ is equal to the 'mean free path' of force chains, and is of order $1/(\rho_d a^{d-1})$ in dimension d. The above equation means the following: since a chain of grains can only transport a force parallel to itself [35], the direction of the force $\vec{n}$ also gives the local direction of the chain. Between $\vec{r}$ and $\vec{r}+\vec{n}\,dr$, the chain can either carry on undisturbed, or be scattered. The second term on the right hand side therefore gives the probability that a force chain initially in direction $\vec{n}'$ is scattered in direction $\vec{n}$. This occurs with a probability $\frac{dr}{\lambda}\Psi(\vec{n}',\vec{n})$, where Ψ is the scattering cross section, which we will assume to depend only on the scattering angle θ, for example a uniform distribution between $-\theta_M$ and $+\theta_M$. The δ-function ensures force conservation and the factor two comes from the counting of the two possible outgoing force chains. Let us now multiply equation (98) by f and integrate over f. This leads to an equation for the local average force per unit volume in the direction $\vec{n}$, that we will denote $F(\vec{n},\vec{r})$. This equation reads:

$$\lambda\,\vec{n}\cdot\vec{\nabla}_r F(\vec{n},\vec{r}) = -F(\vec{n},\vec{r}) + \int d\vec{n}'\,\frac{F(\vec{n}',\vec{r})}{\vec{n}\cdot\vec{n}'}\,\Psi(\vec{n}',\vec{n}) + \frac{\lambda}{a}\,\vec{n}\cdot\vec{F}_0(\vec{r}), \tag{99}$$

where we have added the contribution of an external body force density $\vec{F}_0(\vec{r})$, and a is the size of a defect or of a grain. This equation is the so-called Schwarschild-Milne equation for radiative transfer, describing the evolution of light intensity in a turbid medium [142]. We now introduce some angular averages of $F(\vec{n},\vec{r})$ that have an immediate physical interpretation:

$$p(\vec{r}) = a\int d\Omega\, F(\vec{n},\vec{r}) \tag{100}$$

$$J_\alpha(\vec{r}) = a\int d\Omega\; n_\alpha\, F(\vec{n},\vec{r}) \tag{101}$$

$$\sigma_{\alpha\beta}(\vec{r}) = ad\int d\Omega\; n_\alpha n_\beta\, F(\vec{n},\vec{r}), \tag{102}$$

where $\int d\Omega$ is the normalized integral over the unit sphere, that is introduced for a correct interpretation of σ (see equation (106) below). As will be clear from the following, $\vec{J}$ is the local average force chain intensity per unit surface, σ is the stress tensor. Since $\vec{n}^2 = 1$, one finds that Tr $\sigma = dp$, and therefore p is the isostatic pressure. Note that $\vec{J}$ is not the average local force, which is always zero in equilibrium. The fact that $\vec{J}\neq\vec{0}$ comes from the possibility of *orienting* the force chains.

We now integrate over the unit sphere equation (99) after multiplying it by different powers of n_α. Using the fact that $\Psi(\vec{n}',\vec{n})$ only depends on $\vec{n}\cdot\vec{n}'$, a direct integration leads to:

$$\lambda\,\vec{\nabla}\cdot\vec{J} = (a_0-1)p, \tag{103}$$

where a_0 is called the 'albedo' in the context of light scattering [142], and reads:

$$a_0 \equiv \int d\vec{n}\,\frac{\Psi(\vec{n}',\vec{n})}{\vec{n}\cdot\vec{n}'} \geq 1. \tag{104}$$

A second set of equations can be obtained by multiplying by n_α and integrating. Using the fact that $\int d\vec{n}\,\Psi(\vec{n}',\vec{n}) = 1$, it is easy to show that

$$\int d\vec{n}\,\vec{n}\,\frac{\Psi(\vec{n}',\vec{n})}{\vec{n}\cdot\vec{n}'} = \vec{n}'. \tag{105}$$

Therefore, the resulting equation is nothing but the usual mechanical equilibrium relation:

$$\nabla_\beta\sigma_{\alpha\beta} = F_{0\alpha}. \tag{106}$$

This relation in fact only reflects the local balance of forces chains. Now we multiply equation (99) by $n_\alpha n_\beta$ and again integrate. A priori, this introduces a new three index tensor. In order to close the equation, we now make the an assumption that is

usually made in the context of light diffusion, that on large scales the force intensity becomes nearly isotropic [142]. In this case, it is justified to expand $F(\vec{n},\vec{r})$ in angular harmonics and to keep only the first terms:

$$a\,F(\vec{n},\vec{r}) = p(\vec{r}) + d\vec{n}\cdot\vec{J}(\vec{r}) + ... \tag{107}$$

Within this expansion, we finally obtain a 'constitutive' relation between $\sigma_{\alpha\beta}$ and the vector $\vec{J}$. We find:

$$\sigma_{\alpha\beta}|_{\alpha\neq\beta} = \frac{\lambda d^2 K_1}{\left(\frac{da_2-a_0}{d-1}-1\right)}\left(\nabla_\alpha J_\beta + \nabla_\beta J_\alpha\right), \tag{108}$$

and

$$\sigma_{\alpha\alpha} = \frac{\lambda d}{\left(\frac{da_2-a_0}{d-1}-1\right)}\left[2dK_1\,\nabla_\alpha J_\alpha + \left(dK_1 - \frac{a_0-a_2}{(d-1)(a_0-1)}\right)\vec{\nabla}\cdot\vec{J}\right] \tag{109}$$

with $K_1 = 1/d(2+d)$ and $a_2 = \int d\vec{n}\,(\vec{n}\cdot\vec{n}')\Psi(\vec{n}',\vec{n})$. Rather surprisingly, these equations have exactly the canonical form of elasticity theory, provided one identifies the vector $\vec{J}$ with the local displacement, up to a multiplicative factor.

The above stress equations are rather non-trivial because no displacement field is introduced in the above derivation (nor in the numerical model): elastic-like equations are found in a stress-only model. The basic assumption is the existence of local force chains, which have a well defined identity over several grain sizes a, such that $a \ll \lambda$: this is the condition under which the above Boltzmann description of the force chain scattering is justified.

Since the above equations are formally identical to those of classical elasticity, one can show that $\nabla^2 p = 0$, and $\nabla^4 \vec{J} = 0$ [89]. One can therefore in principle compute the response function $G(\vec{r})$ to a localized force at $\vec{r}_0 = 0$ in the z direction, which is given by the standard (one peak) elastic Green's function. But note however that although the above equations are formally those of classical elasticity, there is one crucial difference coming from the fact that $(\sigma_{\alpha\beta})$ and $\vec{J}$ are not independent since they are both related to the same underlying quantity $F(\vec{n},\vec{r})$. This is a very important difference, which appears, for example in the choice of boundary conditions on $\mathcal{B}$ that determines $P(f,\vec{n},\vec{r})|_{\mathcal{B}}$.

C. The role of chain merging

We have mentioned above the fact that the numerical simulation of the full chain scattering model (including both splitting and merging) was restricted to small depths. Similarly, neglecting chain merging altogether cannot be correct on large length scales, since the number of force chains would diverge, leading to an infinite number of force chains with infinitesimal intensity. As shown in [132], the above linearized theory is in fact unstable, and chain merging play a crucial role to make the theory mathematically consistent.

On the other hand, chain merging leads to a non-linear Boltzmann equation which in the general case cannot be solved. Only special cases have, up to now, been amenable to an analytic treatment. For example, if one insists that the force chains can only take six directions a 60^o degrees, with 120^o degree chain splitting and chain merging, the amplitude of the force chains is constant, simply because $2\cos 60 = 1$. In this case, the full probability distribution $P(f,\vec{n},\vec{r})$ boils down to six functions $p_n(\vec{r})$, describing the probability for a force chain to be in one of the six available directions. The result of the full analysis is that, quite surprisingly, the response function evolves back to a two-peak, hyperbolic structure on large length scales! Whether this is due to the particular structure of the model is not yet settled; preliminary results on the eight-fold model [26] suggests that there might actually be a *transition* between a hyperbolic response for sufficiently anisotropic scattering and an elliptic response for isotropic situations. (see [133] for a nice recent discussion). The existence of such a transition would perhaps, as we discuss now, allow one to reconcile the apparently contradictory experimental, numerical and theoretical results.

IX. STATICS OF GRANULAR MATERIALS: CONCLUDING REMARKS AND OPEN QUESTIONS

Let us try to summarize the theoretical situation as follows. If the grains are frictionless, then packings are generically isostatic. If these packings are furthermore 'sufficiently' anisotropic, then the construction of the stress everywhere in the packing can be performed by 'propagating' the stress from one boundary towards the interior of the packing, as one expects for hyperbolic equations. This situation is well captured by the three-leg model introduced above, that indeed leads to hyperbolic equations on large length scales. Correspondingly, numerical simulations of the response function in *anisotropic* packings of frictionless beads indeed display the expected diffusively broadened two-peak structure, at least for the modest sizes that were simulated [78].

However, not all isostatic packings are characterized by a two-peak response function. For example, using *isotropic* isostatic packings built by J.N. Roux, Ph. Claudin and A. Ayadim [1] have found that the average response function is a single hump, qualitatively similar to the elliptic-like response observed experimentally and to the result of the chain splitting model. An example of such packings is shown in Fig. 9, together with the local force chains. This picture makes it obvious that the

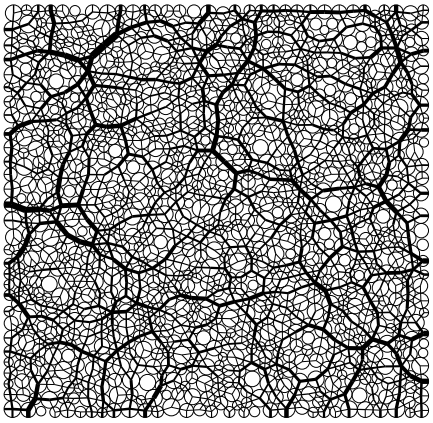

FIG. 9. Force chains in an isotropic, isostatic packing of frictionless disks. The average response function in this case has a single peak. Courtesy of Ph. Claudin.

force chains are strongly scattered, and lose their 'coherence', which makes it indeed plausible that the two-peak structure is destroyed. Again, some degree of anisotropy seems to be required to preserve hyperbolicity. Note that in the numerical determination of the response function, the applied force perturbation δf is infinitesimal and does not induce any rearrangement of the initial structure.

This remark is important since *if* rearrangements are allowed, the response has been argued in [118] to be, on general grounds, elliptic. Moreover, one expects that for any small perturbation, a sufficiently large assembly of frictionless grains will rearrange [44]. Therefore, the order in which the limits $H \to \infty$ and $\delta f \to 0$ are taken is physically relevant [119,79], and one might expect that even anisotropic structures such as those studied in [78] should destabilize under a small perturbation for large enough H. It is not clear which of the limits is relevant in the experimental conditions of [116]; even if the applied force is very small and much care has been devoted to perturb as weakly as possible the packing, it might well be that these experiments are not in the infinitesimal limit.

Conversely, is isostaticity needed to obtain hyperbolicity? The numerical simulations of [63,28], where an hyperbolic response function for anisotropic ordered packing of grains with friction is observed, show that this is not the case. Similarly, the experimental determination of hyperbolic like response function in ordered lattices [103,69] shows that, as suggested by the above theoretical analysis, weak disorder does not suppress the hyperbolic nature of the force propagation. It would be extremely important, in this context, to confirm theoretically the existence of a true 'hyperbolic-elliptic' phase transition in simplified models of force chain scattering.

More formal approaches have also been advocated in [62,2] to try to establish some closure relations between the components of the (coarse-grained) stress tensor starting from the equilibrium force balance at the grain level. Tkachenko and Witten [138] have insisted on the equivalence between any macroscopic linear relation between the components of the stress tensor and the existence of 'floppy' modes, i.e. zero energy deformation modes (see also [102]). Such floppy modes can exist in certain elastic spring networks, such as a square lattice which can deform at no cost along its diagonal. One can indeed show that the large scale elasticity equations in this case are characterized by coefficients such that the marginal condition $r^2 = t$ (see Eq. (54) above) is satisfied, so that the response function becomes the sum of two delta peaks [110]. Following this line of thought, a natural conjecture is that if a system has some *extended* floppy modes, then its large scale response will be hyperbolic. Conversely, if floppy modes are all localized, then the response is locally hyperbolic, but the strong force chain scattering disrupts the long range propagation and the response becomes elliptic like, as suggested by the force chain scattering model discussed above. We hope that these issues will be clarified in the near future; a particularly important point is to establish precisely, starting from a microscopic description à la Edwards, which kind of large scale static equation emerge and under what conditions it is hyperbolic/elliptic, and the value of the parameters entering these equations.

X. GLASSY DYNAMICS IN GRANULAR MEDIA: A BRIEF SURVEY

A. Slow compaction

We have spent quite a long time on the static properties of granular media. The dynamics of *weakly tapped* assemblies of grains is also an extremely interesting subject, in particular in relation with the dynamics of other glassy systems, such as super-cooled liquids, colloidal glasses and foams. The most obvious experiment (with important industrial applications) is that of compaction under tapping. The basic experiment consists in studying the volume occupied by a large number of grains when the container is 'tapped', i.e. subject to a periodic acceleration of a certain amplitude. The packing, initially very loose, progressively compacts. However, the compaction process slows down with time, and the decay of the volume is very far from being a simple exponential. Experiments have shown that the decay of the volume towards its asymptotic value can be satisfactorily fitted by an inverse logarithm of time, or by a stretched exponential, both forms being typical of relaxation processes in glasses, where one can also study the time dependence of the volume (or of the energy) as the sample relaxes after a temperature quench. The parameters of these fits depend on the tapping amplitude – stronger tapping obviously leads to a faster compaction.

More complex experimental protocols have also been tested. For example, one can change, in the course of the experiment, the amplitude of the tapping and reveal interesting memory effects, again similar to those found in glasses and spin-glasses. The now classic experiment [108] is to start from a loose sample and increase slowly the tapping amplitude Γ, in such a way that for each tapping amplitude the density ρ appears to reach a saturation value. One finds that $\rho(\Gamma)$ increases with Γ. When Γ is reduced back to zero, the density keeps a high value, revealing a kind of irreversibility that also appears in spin-glasses under a magnetic field: when the temperature is increased the (zero field cooled) magnetization increases, but does not follow the same path on the way back. The temperature at which the two branches separate is the spin-glass transition temperature (which, if defined in this way, weakly depends on the heating/cooling rate). Similarly, there appears to be a tapping amplitude beyond which the two density branches meet. The high magnetization (field cooled) branch, as the high density branch in the granular system, *is* reversible. As in spin-glasses, the low density branch is in fact out-of-equilibrium, but the convergence of the density (magnetization) towards its equilibrium value is much too slow to be observed.

In the first stage of another type of experiment [83], aimed at revealing 'memory effects', one taps the system with three different amplitudes – say weak, moderate and strong – during a time chosen such as to reach a certain density, identical in the three cases. In the second stage of the experiment, the tapping amplitude is then chosen to be moderate, and the density just after the amplitude 'jump' is observed. If the state of the system was only described by the density, the evolution of the density after the jump should be identical for all three situations, and follow the 'moderate' curve, which is taken as the reference. This is not the case: the weakly tapped system first has to *dilate* before it is able to resume its compaction, whereas the strongly tapped system compacts faster than the reference system just after the jump. This shows that the configurations reached under stronger tapping are in a sense easier to compact further. This experiment therefore indicates that some further 'hidden' observables are needed to describe the large scale evolution of the system. We shall expand on this below, but want to note that a very similar effect is known in glasses as the Kovacs (or memory) effect. In this case, one prepares the system at a given temperature $T_2 < T_1$ and waits until the volume has reached the equilibrium volume at T_1. Then one raises the temperature to T_1. If the volume was the only relevant quantity, one should not see any further evolution since this volume is already at its equilibrium value. Again, this is not what Kovacs first observed in polymeric glasses [84]: the volume has to increase back to a maximum before decreasing again towards its equilibrium value. A similar effect was also reported in numerical simulations of spin-glasses [9] and of Lennard-Jones systems [12], and several simple models are now known to reproduce this effect (see below).

We also want to mention the very interesting experiment of d'Anna et al. [48], where a torsion oscillator is immersed in a vibrated granular assembly. The observable is the angle θ made by the oscillator with an arbitrary axis. The results of [48] are that (a) the angle θ performs a random walk in time: $\langle[\theta(t+\tau)-\theta(t)]^2\rangle = D(\Gamma)\tau$ and (b) the angular diffusion constant $D(\Gamma)$ appears to vanish as the amplitude of the tapping Γ goes to zero in a way that recalls the 'super-activated' Vogel-Fulcher law in glasses.

B. Self-inhibitory dynamics and dynamical heterogeneities

1. Non exponential relaxation

We shall call ρ^* the maximum compacity that can be reached in a tapping experiment. For $\Gamma \to 0$, this corresponds to the so-called 'random close packing' configuration. [It is not entirely clear how meaningful this notion really is, but from an empirical point of view, any reasonable extrapolation of the accessible dynamics seems to converge to a density which is not the HCP density (in the case of identical spheres).] Correspondingly, we will call the difference between ρ^* and the average density ρ the 'free volume' fraction, Φ. The simplest relaxation equation for Φ is obviously a rate equation:

$$\frac{d\Phi}{dt} = -\gamma\Phi. \tag{110}$$

If the decay rate γ is independent of the free-volume itself, the decay of Φ is obviously a single exponential. However, it is intuitively clear that the dynamics is self inhibitory, in the sense that it is the free volume itself that allows further compaction. Therefore, one expects that γ vanishes as $\Phi \to 0$. Assuming a power-law dependence $\gamma \sim \Phi^\beta$, with $\beta > 0$, one obtains a power-law relaxation for long times:

$$\Phi \sim (t + t_0)^{-1/\beta}. \tag{111}$$

Let us assume a simple model where particles have a volume v, and mobile holes have fixed 'quantum' volume v_0. For a particle to be able to move, we require that n^* holes meet in a volume v, such that the volume of one particle is liberated, i.e. $n^* v_0 = v$. If the dynamics is sufficiently chaotic, it is reasonable to assume a Poisson distribution for the holes. Therefore, the probability for a particle to move is simply Φ^{n^*}, leading to $\beta = n^*$. If the number of holes n^* needed to move one particle is large, one can approximate the long time behaviour of Φ as a logarithm:

$$\Phi \sim t^{-1/\beta} \approx \frac{1}{1 + \frac{1}{n^*}\log t}, \tag{112}$$

a form often advocated to fit the slow relaxation of the volume in glasses or granular media [135,108] (but see also [111], where the role of convection is discussed, and [137] for a simple soluble model).

2. Dynamical heterogeneities

If one assumes that holes cannot spontaneously appear, it is clear that the dynamics is necessarily spatially heterogeneous: regions rich in holes, where dynamics is locally fast, appear only to the detriment of regions poor in holes, where the system is jammed. This argument can be somewhat formalized to suggest that the geometry of the 'fast' objects is non trivial. Call $\Phi + \phi(\vec{r}, t)$ the coarse-grained density of free volume ('holes') around point $\vec{r}$ at time t, such that the space average of $\phi(\vec{r}, t)$ is equal to 0. [Note that all 'voids' do not necessarily contribute to the *free* volume]. Far from the boundaries of the sample where the holes can disappear, one can write a Langevin equation for $\phi(\vec{r}, t)$ which reads [51]:

$$\frac{\partial\phi}{\partial t} = D\nabla^2\phi + \vec{\nabla}\cdot[\sqrt{\Phi + \phi}\,\vec{\xi}(t)], \tag{113}$$

where D is the (fast) diffusion constant of the holes, $\vec{\xi}$ is a Gaussian white noise in space and time of variance equal to D, and we have neglected the interaction between the holes. In the above equation, we have supposed that the free-volume is locally conserved. Assuming that ϕ is small leads to the result that ϕ itself is a Gaussian field with a correlation function given (in three dimensions) by:[6]

$$\langle\phi(\vec{r}, t)\phi(\vec{r}', t + \tau)\rangle = \frac{\Phi}{2}\frac{1}{(4\pi D\tau)^{3/2}}\exp\left(-\frac{(\vec{r} - \vec{r}')^2}{4D\tau}\right) \qquad (\tau \geq 0). \tag{114}$$

Note that in the limit $\tau \to 0$, the field ϕ is delta-correlated in space; some short scale cut-off of the order of the grain size a would be needed to regularize this behaviour. Now, if one insists that the material particles (or grains) can only move if the local density of holes is larger than a certain threshold Φ_c, the diffusion equation for, say, the density $\rho(\vec{r}, t)$ of slow tracer particles reads (see also [94] for similar ideas):

$$\frac{\partial\rho}{\partial t} = D_0\vec{\nabla}\cdot\left[\Theta(\Phi + \phi - \Phi_c)\vec{\nabla}\overline{\rho}\right]. \tag{115}$$

Although a more careful solution of the coupled equations (113, 115) is required to confirm the following conclusions, a qualitative analysis of the problem leads to the following picture for glassy dynamics, which relates slow, self-inhibitory dynamics and dynamical heterogeneities:

- The probability that an elementary region of space is active is, for small $\Phi \ll \Phi_c$, proportional to $\exp(-C\Phi_c^2/\Phi)$, where C is a numerical coefficient. Therefore, the large scale diffusion coefficient D_R of the particles vanishes as:

$$D_R \sim D_0\exp\left(-\frac{C\Phi_c^2}{\Phi}\right) = D_0\exp\left(-\frac{C\Phi_c^2}{\rho^* - \rho}\right), \tag{116}$$

  i.e. à la Vogel-Fulcher. This argument is actually the analogue of the classic free-volume argument leading to the Vogel-Fulcher law in glasses, and extended to granular media by Boutreux and De Gennes [27].

---

[6] If one considers that 'holes' can be converted into voids and vice-versa, such that ϕ is only conserved on average, the statistics of the ϕ field is altered and becomes that of an elastic membrane subject to thermal fluctuations.

- The fast regions are delimited by the contour lines of a correlated Gaussian field. This has interesting consequences: for example, one expects, in the short-ranged conserved case, the active regions to be lattice animals of fractal dimension $d_f = 2$ in three dimension (and $d_f \approx 1.56$ in two dimensions). The value $d_f = 2$ turns out to be in agreement with the experimental determination of Weeks et al. on dense, three dimensional colloidal glasses [144]. It would be interesting to measure other geometrical characteristics of the fast clusters to confirm that these are indeed lattice animals (see e.g. the discussion in [88]). Interestingly, the connection between glassy dynamics and the contour lines of a dynamic random field was also suggested in [36], using rather different arguments.

It would be most interesting to make these statements more precise in the context of a specific model. Very promising steps in that directions have been made recently in dynamically constrained models [67,139,117].

As emphasized by Boutreux and De Gennes, a Vogel-Fulcher law such as Eq. (116) also leads to a logarithmic relaxation of the density. Indeed, writing:

$$\frac{d\Phi}{dt} = -\gamma_0 \exp\left(-\frac{C\Phi_c^2}{\Phi}\right)\Phi, \tag{117}$$

leads at large times to:

$$\Phi \approx \frac{C\Phi_c^2}{\log t}. \tag{118}$$

3. Another point of view: Edwards postulate

The above Vogel-Fulcher law can also be understood using Edwards' analogy with thermodynamics. Assume again that all blocked states are equiprobable. Then the states that are most likely to be observed are the most numerous ones: this is the essence of statistical thermodynamics. Imagine for example that a container is divided by a movable piston, with grains in each compartments. The volume of the two compartments are V_1 and V_2, with $V_1 + V_2 = V$. The Edwards entropy $\mathcal{S}$ is the logarithm of the number of blocked states for a given overall volume. The total entropy of the container is:

$$\mathcal{S}_T = \mathcal{S}_1 + \mathcal{S}_2. \tag{119}$$

The most probable value of V_1 is such that this entropy is maximum, under the constraint $V_1 + V_2 = V$. Therefore, one has:

$$\frac{\partial \mathcal{S}_1}{\partial V_1} = \frac{\partial \mathcal{S}_2}{\partial V_2}. \tag{120}$$

In thermodynamics, this quantity (which is constant throughout the system) is equal to P/T, where P is the pressure. In the context of granular materials, $\partial\mathcal{S}/\partial V > 0$ was called the inverse compactivity by Edwards, and noted $1/X$.

A reasonable requirement for $\mathcal{S}(V)$ is that it should be proportional to the number of grains N, and only depends on the free-volume fraction Φ: $\mathcal{S}(V) = Ns(\Phi)$. One also expects that $s(\Phi)$ vanishes for $\Phi \to 0$. A possibility, suggested in [65,91], is that each grain has a number of possible positions proportional to the free-volume, which leads to $s(\Phi) = \log \Phi/\upsilon_0$, where υ_0 is again a 'quantum' of free-volume. Using this form for $s(\Phi)$, we finally find:

$$\frac{\partial \mathcal{S}}{\partial V} = \frac{1}{X} = \frac{N^2\upsilon}{V^2}\frac{\partial s}{\partial \Phi} \approx \frac{\rho^{*2}\upsilon}{\Phi} \qquad (\Phi \ll 1), \tag{121}$$

showing that the Edwards 'temperature' vanishes for $\Phi \to 0$.[7] Now, consider a small region immersed in a large container with grains, which acts as a reservoir of free volume. Exactly as in thermodynamics, one can show that the probability that a free-volume equal to v is found in this region is given by:

$$p(\mathrm{v}) \propto \exp(-\frac{\mathrm{v}}{\mathrm{X}}) \tag{122}$$

The probability for a hole of the size of a grain υ to appear is therefore: $p(\mathrm{v} = \upsilon) \sim \exp(-\Phi^{*2}/\Phi)$, where $\Phi^* \equiv \rho^*\upsilon$. Assuming that the grain motion takes place when a sufficiently large hole appears, one finds that the rate of compaction has the same exponential form as above.

---

[7] Note the following intriguing consequence of Edwards postulate. Suppose that the two compartments contain grains of the very same material, but with different sizes (volume) υ_1 and υ_2, such that $N_1\upsilon_1 = N_2\upsilon_2$, i.e. the volume fraction occupied by the grains in the two compartments is the same. The equality $X_1 = X_2$ then imposes that $\Phi_1/\Phi_2 = \upsilon_2/\upsilon_1$, i.e. that smaller grains will have a higher free volume. This conclusion holds for more general choices of the entropy $s(\Phi)$.

C. Granular dynamics and the trap model

The above 'free-volume' ideas are interesting and certainly contain important physical ideas. However, the description of the dynamics using a single macroscopic degree of freedom (namely the average free volume density) is too naive to account for the more sophisticated 'memory' experiments. Indeed, any rate equation of the form:

$$\frac{d\Phi}{dt} = -\gamma(\Phi, \Gamma)\Phi, \tag{123}$$

is unable to explain why a packing prepared under different tapping conditions (different Γ), but such as to reach the same value Φ_0 would evolve differently if tapped with the same amplitude. The same argument was used by Kovacs in the context of glasses to suggest that additional parameters are needed to fully describe a glassy state. Take the example of a one dimensional ferromagnetic Ising model that relaxes towards its equilibrium state a temperature T. Since the system does not order, the equilibrium state is characterized by a density of domain walls (or kinks), defining a characteristic domain size, which is the distance between the kinks. The non equilibrium state can also be characterized by a density of kinks, which decays with time towards the equilibrium. However, the full description of the non equilibrium state requires the specification of the *distribution* of the domain size – only its first moment is fixed by the average density of kinks. Different initial distributions of domain sizes with the same average value do evolve differently at a given temperature. For example, if there is an initial excess probability of large domains (but such that the density of kinks is the equilibrium one), these will immediately break down, leading to a temporary increase of the density of kinks.

A simple model that encapsulates both the spatial heterogeneity and the intermittency of the dynamics, is the 'trap' model. One should think of a glassy system as made of independent subsystems of a certain size ξ (see Fig. 10). Inside each of these regions, the dynamics is 'coherent' in the sense that hopping between different metastable states involves all particles within a blob of size $\leq \xi$. Within each of these subunits, the dynamics can be thought of as a random walk in a rugged landscape, an idea with a long history in the context of glasses [74], and witnessing a strong recent revival in different contexts [85,37,75]. However, an element which often seems to be missing from the discussion is the fact that the dynamics of system *as a whole* necessarily results (for short range interactions) from the evolution in parallel of many subsystems: the dynamics of a particle in a given subregion is completely unaffected by the dynamics of far away particles. An open problem is to identify precisely the (possibly time dependent) coherence length ξ, and understand its temperature and density dependence (see [55] for very interesting results on this aspect in the context of Lennard-Jones systems).

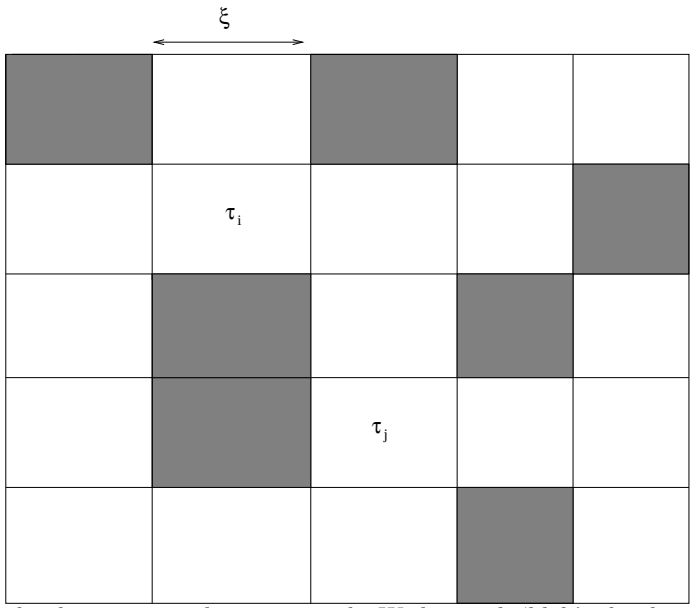

FIG. 10. Schematic view of the dynamics in glassy material. Within each 'blob', the dynamics is 'coherent' in the sense that hopping between different metastable states involves all particles within a blob of size $\leq \xi$, whereas the motion of far away particles does not affect the dynamics within this blob. Within each of these subunits, the dynamics can be thought of as a random walk in a rugged landscape, with an instantaneous (random) trapping time τ_i in the ith blob. Grey regions are particularly 'slow' ($\tau \gg t_w$).

The dynamics of a given subsystem can be seen as a succession of hops between different metastable states, each of which blocking the dynamics for a time that depends on the local packing fraction: high densities leads to long trapping times. The

state of the system at time t is described by a *probability distribution* $P(\phi,t)$, which counts the number of subsystems with a local value ϕ of the free volume. Each time a subunit unjams, we assume that it falls back into any of the blocked states with an *a priori* distribution $P_0(\phi)$, that reflects the number of states with a given packing density. The time evolution of $P(\phi,t)$ is then given by:

$$\frac{dP(\phi,t)}{dt} = -\frac{1}{\tau(\phi)}P(\phi,t) + \left\langle \frac{1}{\tau(\phi)} \right\rangle_t P_0(\phi). \tag{124}$$

This equation was introduced in [58,20,100] in the context of glasses, and extended to granular media by D. Head [77], where the free volume density ϕ plays the rôle of the energy E. This equation neglects any coupling between nearby sub-systems. This is obviously unrealistic since the free volume liberated at one point will in general help nearby volumes to unjam. A generalization of the above model that takes into account, to some extent, this coupling, can be found in [20,100,76].

The trap model, and its 'SGR' (Soft Glassy Materials) generalisation covered in Mike Cates lectures [134,66], exhibits a number of interesting features, such as a genuine glass transition, aging and non linear rheology. A crucial ingredient of the trap model is the possibility for the average trapping time to diverge. Taking $\tau(\phi) \sim \exp(A/\phi)$, where A is a certain constant that may depend on the tapping amplitude Γ, and $P_0(\phi) = \exp[\xi^3 s(\phi)]$ with $s(\phi) = B\log\phi$, we find that the distribution of trapping times $\Psi(\tau)$ decays very slowly, as $1/\tau(\log\tau)^a$, where $a = 2 + B\xi^3$. This means that one is always in the glassy phase of the trap model, since $\langle\tau\rangle = \infty$.[8] Correspondingly, one expects not only slow (logarithmic) compaction but also aging effects, such as reported in numerical simulations [107]. In the glassy phase, the trap model describes the dynamics of each subsystem as essentially *intermittent*: either the system is blocked, or it moves fast to a quite different configuration; most of the time is spent in one particularly well jammed configuration. This intermittent dynamics of glassy systems begins to have some numerical [54,53,10] and experimental [120,32,39] support. However, one should remember that if one looks at the system as a whole, the activity will be dominated by the fastest regions (which can in turn, through the coupling between nearby that we have neglected above, unlock the slow regions).

Interestingly, the trap model is able to reproduce some of the cycle effects reported above: the irreversibility in a tapping cycle [77], or the Kovacs effect [12,143]. Variants of the trap model can also be studied, where each 'trap' is decorated by the dynamics of smaller length scales [17,23] in order to account for memory and rejuvenation effects observed in spin-glasses and other glassy systems. The Sinai model is in this family of 'multi-scale' trap models [87,90,121], and was introduced in the context of granular media precisely to understand the memory and cycle effects [95], although the simpler 'monoscale' trap model seems to be able to account for most of them. It would be very interesting to exhibit experimentally a truly 'multiscale' dynamical phenomenon in granular materials. This would have the obvious advantage over many other glassy systems that the underlying mechanism, in terms of embedded length scales, can be directly observable [23,25].

There would be much more to say about glassy dynamics in the context of granular materials, but my lectures stopped at this point, after only quite simple ideas were expressed. Since some of the more elaborated concepts are common to spin-glass dynamics and glassy rheology, it is appropriate to refer to the lectures of Mike Cates, Leticia Cugliandolo and Giorgio Parisi in this volume, and also to [11,92,22,6] for further developments.

---

[1] A. Ayadim, Ph. Claudin, J. N. Roux, unpublished.
[2] R.C. Ball and R. Blumenfeld, Phys. Rev. Lett. **88**, 115505 (2002).
[3] A. Barrat, J. Kurchan, V. Loreto, M. Sellitto, Phys. Rev. Lett. **85** 5034 (2000)
[4] A. Barrat, V. Colizza, V. Loreto, Phys. Rev. E **66** 011310 (2002); Phys. Rev. E **65**, 050301 (2002)
[5] J. Berg, S. Franz, M. Sellitto, Euro. Phys. J. **B 26**, 349 (2002)
[6] L. Berthier, L. Cugliandolo, J.L. Iguain, Phys. Rev. **63**, 051302 (2001).
[7] L. Berthier and P. C. W. Holdsworth, Europhys. Lett. **58**, 35 (2002).
[8] L. Berthier, J.-L. Barrat, Phys. Rev. Lett. **89** 095702 (2002)
[9] L. Berthier and J.-P. Bouchaud, Phys. Rev. B **66**, 054404 (2002).
[10] L. Berthier, *Yield stress, heterogeneities and activated processes in soft glassy materials*, preprint cond-mat/0209394.
[11] L. Berthier, V. Viasnoff, O. White, V. Orlyanchik, F. Krzakala, this volume.
[12] E. Bertin, J. P. Bouchaud, J.M. Drouffe, C. Godrèche, in preparation.
[13] D. Blair, N. Mueggenburg, A. Marshall, H. Jaeger, and S. Nagel, Physical Review E **63**, 041304 (2001).

[8] Note that the logarithmic tail found above can be seen as an effective power-law with a time dependent effective exponent $\mu = a/\log\tau$. This suggests that the relevant coherence length after time t is such that $B\xi^3 \sim \log t$.

[14] R. Blumenfeld, S. F. Edwards, R. C. Ball, *Granular Matter and the Marginal Rigidity State*, preprint cond-mat/0105348.
[15] D. Bonamy, PhD. Thesis, unpublished (2001).
[16] D. Bonamy, F. Daviaud, L. Laurent, M. Bonetti and J.P Bouchaud, Phys. Rev. Lett. **89**, 034301 (2002).
[17] J.-P. Bouchaud, D.S. Dean, J. Phys. I (France) **5**, 265 (1995).
[18] J.-P. Bouchaud, M.E. Cates and P. Claudin, J. Phys. I (France) **5**, 639 (1995).
[19] J.-P. Bouchaud, L. Cugliandolo, J. Kurchan, M. Mézard, Physica **A226**, 243 (1996).
[20] J. P. Bouchaud, A. Comtet, C. Monthus, J. Phys. I France **5** 1521 (1995).
[21] J.-P. Bouchaud, P. Claudin, M.E. Cates, J.P. Wittmer, in *Physics of Dry Granular Media*, H.J. Herrmann, J.P. Hovi and S. Luding, Eds., NATO ASI, 97 (1997).
[22] J.-P. Bouchaud, L. Cugliandolo, J. Kurchan, M. Mézard, in *Spin-glasses and Random Fields*, edited by A. P. Young (World Scientific, Singapore, 1998), and references therein.
[23] J.-P. Bouchaud, in *Soft and Fragile Matter*, edts: M. E. Cates and M.R. Evans (Institut of Physics Publishing, Bristol and Philadelphia, 2000).
[24] J.P. Bouchaud, P. Claudin, D. Levine, and M. Otto, Eur. Phys. J E **4**, 451 (2001).
[25] J.-P. Bouchaud, V. Dupuis, J. Hammann, E. Vincent, Phys. Rev. B **65**, 024439 (2002).
[26] J.P. Bouchaud, P. Claudin, M. Otto, J.E.S. Socolar, in preparation.
[27] T. Boutreux, P. G. de Gennes, Physica A **244**, 59 (1997)
[28] L. Breton and E. Clément and P. Claudin and J.-D. Zucker, to appear in Europhys. Lett.
[29] R. Brockbank, J.M. Huntley, and R.C. Ball, J. Phys. II (France), **7**, 1521-1532 (1997).
[30] R.L. Brown and J.C. Richard, 'Principles of Powder Mechanics' (Pergamon, New York, 1966).
[31] J. Brujic, S. F. Edwards, I. Hopkinson, H. A. Maakse, *Characterisation of the micromechanics in a compressed emulsion system: Force distribution*, preprint cond-mat/0210136.
[32] L. Buisson, L. Bellon and S. Ciliberto, *Intermittency in Aging*, preprint.
[33] F. Cantelaube and J. D. Goddard, in *Powders and Grains 97*, Behringer and Jenkins eds., Balkema, Rotterdam (1997), p. 231-234.
[34] M.E. Cates, J.P. Wittmer, J.-P. Bouchaud and P. Claudin, Phil. Trans. Roy. Soc. Lond. A **356**, pp 2535-2560 (1998).
[35] M.E. Cates, J.P. Wittmer, J.-P. Bouchaud and P. Claudin, Phys. Rev. Lett. **81**, 1841 (1998).
[36] H. E. Castillo, C. Chamon, L. F. Cugliandolo, J.-L. Iguain, M. P. Kennett. *Spatially heterogeneous ages in glassy dynamics*, e-print cond-mat/0211558.
[37] A. Cavagna, Europhys. Lett. **53**, 490 (2001).
[38] M. Chertkov, G. Falkovich and V. Lebedev, Phys. Rev. Lett. **76** 3707 (1996) and refs. therein.
[39] L. Cipelletti, H. Bissig, V. Trappe, P. Ballestat, S. Mazoyer, submitted to J. Phys. Cond. Mat.
[40] P. Claudin and J.-P. Bouchaud, Phys. Rev. Lett. **78**, 231 (1997), and this volume.
[41] P. Claudin, J.-P. Bouchaud, M.E. Cates and J.P. Wittmer, Phys. Rev. E **57**, 4441 (1998).
[42] P. Claudin, Ann. de Physique, **24**, 1 (1999).
[43] E. Clément, G. Reydellet, L. Vanel, D.W. Howell, J. Geng and R.P. Behringer, XIIIth Int. Cong. on Rheology, Cambridge (UK), vol. 2, 426 (2000).
[44] G. Combe and J.-N. Roux, Phys. Rev. Lett. **85**, 3628 (2000).
[45] A. Coniglio, A. Fierro, M. Nicodemi, *Probability distribution of inherent states in models of granular media and glasses*, preprint cond-mat/0206275.
[46] S.N. Coppersmith, C.-h. Liu, S. Majumdar, O. Narayan and T.A. Witten, Phys. Rev. E **53**, 4673 (1996).
[47] D. Cule and Y. Shapir Phys. Rev. **B50** 5119 (1994).
[48] G. D'Anna, P. Mayor, G. Gremaud, A. Barrat, V. Loreto, *Extreme events driven glassy behaviour in granular media*, Europhys. Lett., to appear, e-print cond-mat/0210263.
[49] P. Dantu, Ann. des Ponts et Chaussées **4**, 144 (1967).
[50] O. Dauchot, private communication and in preparation.
[51] D. S. Dean, J. Phys A **29**, L613 (1996).
[52] D. S. Dean, A. Lefevre, Phys. Rev. Lett. **86**, 5639 (2001).
[53] R. A. Denny, D. R. Reichman, J.-P. Bouchaud, *Trap Model and Slow Dynamics in Supercooled Liquids*, preprint cond-mat/0209020.
[54] B. Doliwa, A. Heuer, *Hopping in a Supercooled Lennard Jones liquid: Metabasins, Waiting-time distribution and Diffusion*, preprint cond-mat/0205283.
[55] B. Doliwa, A. Heuer, *Energy Barriers and Activated Dynamics in a Supercooled Lennard-Jones Liquid*, preprint cond-mat/0209139.
[56] J. Duran, *Sables, poudres et grains*, Eyrolles Sciences, Paris (1997), Springer, New-York (2001).
[57] J. Duran, J.P. Bouchaud (Edts), *Physics of Granular Media*, Comptes Rendus de l'Academie des Sciences (Special Issue), **3**, 129 (2002).
[58] J.C. Dyre, Phys. Rev. Lett. **58**, 792 (1987); Phys. Rev. B **51**, 12 276 (1995).
[59] S.F. Edwards and R.B. Oakeshott, Physica D **38**, 88 (1989).
[60] S. F. Edwards, R. B. S. Oakeshott, Physica A **157** 1080 (1989), S. F. Edwards, in *Disorder in Condensed Matter Physics*,

Oxford Science Publications (1991).
[61] S.F. Edwards and C.C. Mounfield, Physica A **226**, 1,12,25 (1996).
[62] S.F. Edwards and D.V. Grinev, Phys. Rev. Lett **82**, 5397 (1999); S.F. Edwards, D. Grinev, Physica A **294**, 57 (2001).
[63] C. Eloy and E. Clément, to appear in J. Phys. I (France) (1997).
[64] D. Ertas, T. Halsey, Phys. Rev. Lett. **83**, 5007 (1999).
[65] M.L. Falk, J. S. Langer, M.R.S. Bulletin **25**, 40 (2000).
[66] S.M. Fielding, P. Sollich, M.E. Cates, J. Rheol **44**, 323 (2000).
[67] J.P. Garrahan, D. Chandler, *Geometrical explanation and scaling of dynamical heterogeneities in glass forming systems*, preprint cond-mat/0202392.
[68] C. Gay, R. da Silveira, cond-mat/0208155. R. da Silveira, G. Vidalenc and C. Gay, cond-mat/0208214.
[69] J. Geng, D. Howell, E. Longhi, R.P. Behringer, G. Reydellet, L. Vanel, E. Clément and S. Luding, Phys. Rev. Lett. **87**, 035506 (2001), J. Geng, G. Reydellet, E. Clément, R. P. Behringer, *Green's Function Measurements in 2D Granular Materials*, preprint cond-mat/0211031
[70] P.-G. de Gennes, Collège de France lectures, unpublished (1995).
[71] P.-G. de Gennes, Rev. Mod. Phys. **71**, S374 (1999).
[72] I. Goldhirsch, in [80]
[73] C. Goldenberg and I. Goldhirsch, Phys. Rev. Lett. **89**, 084302 (2002).
[74] M. Goldstein, J. Chem. Phys. **51**, 3728 (1969)
[75] T.S. Grigera, A. Cavagna, I. Giardina, G. Parisi, Phys. Rev. Lett, **88** 055502 (2002) and refs. therein.
[76] D. Head, J. Phys. A **33** 465 (2000)
[77] D. Head, Phys. Rev. **E 62**, 2439 (2000)
[78] D. Head, A. Tkachenko, and T. Witten, European Physical Journal E **6**, 99 (2001).
[79] D. Head, A. Tkachenko, and T. Witten, European Physical Journal E **7**, 299 (2002).
[80] H.J. Herrmann, J.P. Hovi and S. Luding (Edts.), *Physics of Dry Granular Media*, NATO ASI, 25 (1997)
[81] H.M. Jaeger, S. R. Nagel, R. P. Behringer, Rev. Mod. Phys. **68**, 1259 (1996)
[82] H.A. Janssen, *Z. Vert. Dt. Ing.* **39**, 1045 (1895); see also [106].
[83] Ch. Josserand, A. Tkachenko, D. M. Mueth, H. M. Jaeger, Phys. Rev. Lett. **85** 3632 (2000)
[84] A. J. Kovacs, Adv. Polym. Sci. **3**, 394 (1963); A. J. Kovacs *et al.*, Journal of Polymer Science **17**, 1097 (1979).
[85] J. Kurchan, L. Laloux, J. Phys. **A29**, 1929 (1996)
[86] J. Kurchan, in [92].
[87] L. Laloux and P. Le Doussal, Phys. Rev. E **57** 6296 (1998),
[88] J. Lamarcq, J. P. Bouchaud, O. Martin, M. Mézard, Europhys. Lett. **58**, 321 (2002).
[89] L. D. Landau, E. M. Lifshitz, *Theory of Elasticity*, 3rd Edn., Pergamon, Oxford 1986
[90] P. Le Doussal, C. Monthus, D. S. Fisher, Phys. Rev. E **59** 4795 (1999).
[91] A. Lemaitre, *A dynamical approach to glassy materials*, preprint cond-mat/0206417.
[92] A. Liu, S. Nagel (Edts.), *Jamming and Rheology*, Taylor & Francis, 2001.
[93] C.-H. Liu, S.R. Nagel, D.A. Scheeter, S.N. Coppersmith, S. Majumdar, O. Narayan and T.A. Witten, Science **269**, 513 (1995).
[94] D. Long, F. Lequeux, Eur. Phys. J E **4** 371 (2001).
[95] S. Luding, M. Nicolas, O. Pouliquen, in: *Compaction of Soils, Granulates and Powders*, D. Kolymbas and W. Fellin (eds.), A. A. Balkema, Rotterdam (2000)
[96] S. Luding, in [57].
[97] H. A. Maakse, J. Kurchan, Nature, **415**, 614 (2002)
[98] B. Meerson, T. Poeschel, P. V. Sasorov, T. Schwager, *Breakdown of granular hydrodynamics at a phase separation threshold*, preprint cond-mat/0208286
[99] R. Monasson and O. Pouliquen, Physica A **236**, 395 (1997).
[100] C. Monthus, J.-P. Bouchaud, J. Phys. A: Math. Gen. **29**, 3847 (1996).
[101] J.-J. Moreau, in the proceedings of the *colloque 'Physique et mécanique des matériaux granulaires'*, Champs-sur-Marne (France), 199 (2000).
[102] C. F. Moukarzel, Phys. Rev. Lett. **81**, 1634 (1998); *Granular matter instability: A structural rigidity point of view*, preprint cond-mat/9807004.
[103] N. Mueggenburg, H. Jaeger, and S. Nagel, *Stress transmission through three dimensional ordered granular arrays*, cond-mat/0204533.
[104] O. Narayan, S. R. Nagel, Physica A **264** 75 (1999).
[105] O. Narayan, Phys. Rev. E **63**, 10301 (2001).
[106] R.M. Nedderman, *Statics and Kinematics of Granular Materials* Cambridge University Press (1992).
[107] M. Nicodemi, A. Coniglio, H.J. Herrmann, Phys. Rev. E **55**, 3962 (1997)
[108] E. R. Nowak, J. B. Knight, E. Ben-Naim, H.M. Jaeger, S. R. Nagel, Phys. Rev. **E 57**, 1971 (1998)
[109] C. S. O'Hern, S. A. Langer, A. J. Liu, S. R. Nagel, Phys. Rev. Lett. **86**, 111 (2001)
[110] M. Otto, J.P. Bouchaud, P. Claudin, J.E.S. Socolar, preprint cond-mat/0211015.

[111] P. Philippe, D. Bideau, preprint cond-mat/0210297, to appear in Europhys. Lett.
[112] T. Poeschel, S. Luding (Edts), *Granular gases*, Lecture Notes in Physics 564, Springer (Berlin) 2001.
[113] T. Poeschel, N. V. Brilliantov, T. Schwager, *Violation of Molecular Chaos in dissipative gases*, preprint cond-mat/0210058.
[114] F. Radjai, D.E. Wolf, M. Jean, J.J. Moreau, Phys. Rev. Lett. **80**, 61 (1998), and references therein.
[115] R. Rajesh, S. Majumdar, Phys. Rev. **E62**, 3186 (2000).
[116] G. Reydellet and E. Clément, Phys. Rev. Lett. **86**, 3308 (2001).
[117] F. Ritort, P. Sollich, *Glassy dynamics of kinetically constrained models*, e-print cond-mat/0210382.
[118] J. N. Roux, Phys. Rev. **E61** 6802 (2000).
[119] J. N. Roux, European Physical Journal E **7**, 297 (2002).
[120] E. V. Russell, N. E. Israeloff, Nature **408**, 695 (2000)
[121] M. Sales, J.-P. Bouchaud, F. Ritort, e-print cond-mat/0207273, to appear in J. Phys. A.
[122] L. Saul, M. Kardar and N. Read, Phys. Rev. **A45** 8859 (1992)
[123] S. B. Savage in *Powders and Grains 97*, Behringer and Jenkins eds., Balkema, Rotterdam (1997), p. 185-194; see also New Scientist, **2083**, p.28 (1997).
[124] D. Serero, G. Reydellet, P. Claudin, E. Clément, and D. Levine, European Physical Journal E **6**, 169 (2001).
[125] L. E. Silbert, D. Ertas, G. S. Grest, T. C. Halsey, D. Levine, *Geometry of frictionless and frictional sphere packing*, preprint cond-mat/0111140 see also L. E. Silbert, D. Ertas, G. S. Grest, T. C. Halsey, D. Levine, *Granular 'glass' transition*, preprint cond-mat/0109124.
[126] M. da Silva and J. Rajchenbach, Nature **406**, 70 (2000).
[127] G. de Smedt, C. Godrèche, J. M. Luck, Eur. Phys. J. B 27, 363-380 (2002)
[128] J. Smid and J. Novosad, Proc. of 1981 Powtech Conference, Ind. Chem. Eng. Symp. **63**, D3V 1-12 (1981).
[129] J. H. Snoeijer, J. M. J. van Leeuwen, *Force relaxation in the q-model for granular media*, preprint cond-mat/0202120
[130] J. H. Snoeijer, M. van Hecke, E. Somfai, W. van Saarloos, *Effect of boundaries on the force distributions in granular media*, preprint cond-mat/0204277
[131] J.E.S. Socolar, Physical Review E **60**, 1999 (1999).
[132] J.E.S. Socolar, D.G. Schaeffer, P. Claudin, Eur. Phys. J. E **7**, 353 (2002).
[133] J.E.S. Socolar, *Discrete models of force chain networks*, cond-mat/0212162
[134] P. Sollich, F. Lequeux, P. Hebraud and M.E. Cates, Phys. Rev. Lett. **78**, 2020 (1997), S.M. Fielding, P. Sollich, M.E. Cates, J. Rheol **44**, 323 (2000).
[135] L. C. E. Struik, *Physical aging in amorphous polymers and other materials* (Elsevier, Amsterdam, 1978).
[136] H. Takayama, I. Nishikawa, H. Tasaki, Phys. Rev. A *37*, 3110 (1988).
[137] J. Talbot, G. Tarjus and P. Viot, Eur. Phys. J. E **5** 445 (2001).
[138] V. Tkachenko and T.A. Witten, Phys. Rev. E **60**, 687 (1999); Phys. Rev. E **62**, 2510, (2000).
[139] C. Toninelli, G. Biroli and D.S. Fisher, in preparation.
[140] L. Vanel, D.W. Howell, D. Clark, R.P. Behringer and E. Clément, Phys. Rev. E **60**, R5040 (1999)
[141] L. Vanel, P. Claudin, J.-P. Bouchaud, M.E. Cates, E. Clément, and J.P. Wittmer, Phys. Rev. Lett. **84**, 1439 (2000).
[142] M.C.W. van Rossum and Th.M. Nieuwenhuizen, Rev. Mod. Phys. **71**, 313 (1999).
[143] V. Viasnoff, F. Lequeux, Phys. Rev. Lett. **89**, 065701 (2002)
[144] E. R. Weeks, J. C. Crocker, A. C. Levitt, A. Schofield, D. A. Weitz, *Science*, 287, 627 (2000).
[145] J.P. Wittmer, M.E. Cates, P. Claudin and J.-P. Bouchaud, Nature (London) **382**, 336 (1996). J.P. Wittmer, P. Claudin, M.E. Cates, J. Phys. (France) I **7**, 39 (1997).
[146] J.P. Wittmer, M.E. Cates and P. Claudin, J. Phys. I (France) **7**, 39 (1997).
[147] J.P. Wittmer, A. Tanguy, J.-L. Barrat, L. Lewis, *Vibrations of amorphous, nanometric structures: When does continuum theory apply?*, preprint cond-mat/0104509.
[148] D.M. Wood, *Soil Behaviour and Critical State Soil Mechanics*, Cambridge University Press, Cambridge (1990).